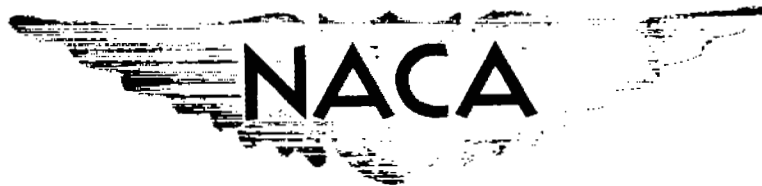


~~CONFIDENTIAL~~Copy  
RM L53C18

6

NACA RM L53C18



# RESEARCH MEMORANDUM

LOW-SPEED INVESTIGATION OF THE AERODYNAMIC, CONTROL, AND  
HINGE-MOMENT CHARACTERISTICS OF TWO TYPES OF  
CONTROLS ON A DELTA-WING—FUSELAGE MODEL  
WITH AND WITHOUT NACELLES

By William I. Scallion

Langley Aeronautical Laboratory  
Langley Field, Va.

~~CLASSIFICATION CANCELLED~~

Approved: *Spaca Rep. 66-113 3/16/56*  
*RM 96*  
By: *27271 3/27/56*

CLASSIFIED DOCUMENT

This material contains information affecting the National Defense of the United States within the meaning of the espionage laws, Title 18, U.S.C., Secs. 793 and 794, the transmission or revelation of which in any manner to an unauthorized person is prohibited by law.

## NATIONAL ADVISORY COMMITTEE FOR AERONAUTICS

WASHINGTON

May 20, 1953

~~CONFIDENTIAL~~

## NATIONAL ADVISORY COMMITTEE FOR AERONAUTICS

## RESEARCH MEMORANDUM

## LOW-SPEED INVESTIGATION OF THE AERODYNAMIC, CONTROL, AND

## HINGE-MOMENT CHARACTERISTICS OF TWO TYPES OF

## CONTROLS ON A DELTA-WING—FUSELAGE MODEL


## WITH AND WITHOUT NACELLES

By William I. Scallion

## SUMMARY

An investigation was made in the Langley full-scale tunnel to determine the low-speed aerodynamic and control characteristics of a 3-percent-thick  $60^\circ$  sweptback delta-wing—fuselage combination with half-delta tip controls and horn-balance-type controls. Tests were also made with chord-plane-mounted nacelles located at three different spanwise positions on the wing. Aerodynamic forces and moments and hinge-moment data were obtained through the angle-of-attack range at a Reynolds number of  $2.3 \times 10^6$  and a Mach number of 0.10.

The longitudinal and lateral control effectiveness of the half-delta and horn-balance-type controls on the model without nacelles decreased at high angles of attack. The horn-balance-type control was approximately twice as effective as the half-delta tip control throughout the angle-of-attack range. The longitudinal and lateral control effectiveness of both controls was improved by installing nacelles adjacent to the controls. Adverse yawing moments were produced by both controls at positive control deflections and angles of attack above  $4.3^\circ$ . The outboard (0.67 semispan) nacelle adjacent to the half-delta tip control caused that control to produce large adverse yawing moments with negative control deflections and high angles of attack. The control hinge moments of the half-delta tip control were small but varied nonlinearly with angle of attack and control deflection. The nacelle mounted adjacent to this control caused a shift from negative to positive hinge moments for negative control deflections. The hinge-moment characteristics of the horn-balance-type control were more nearly linear than those of the half-delta control and large negative values of the rate of change of hinge-moment coefficient with angle of attack and right control deflection  $C_{h\alpha}$  and  $C_{h\delta_r}$  were obtained from this control.



## INTRODUCTION

The present interest in thin delta wings for high-speed aircraft has resulted in a need for considerable information on the control characteristics of such wings over the complete speed range. Recent high-speed investigations on the control and hinge-moment characteristics of various controls on delta wings (refs. 1 to 3) have shown that half-delta tip controls maintain more satisfactory control effectiveness with lower hinge moments than other types of controls at transonic and supersonic speeds. Investigation of the effectiveness of tip controls has been extended to the low-speed range, for example, by references 4 and 5; however, the hinge-moment characteristics of such controls have not been adequately studied in view of the marked variation on tip loading with angle of attack known to exist on highly swept wings subject to leading-edge-separation vortex-type flow. In addition, there is little information on the effects of chord-plane-mounted external stores or nacelles on the characteristics of tip controls; therefore, these effects merit study in view of the influence of such nacelles on the leading-edge vortex and low-speed stall characteristics as indicated by reference 6.

As part of a program of investigation of the low-speed aerodynamic and control characteristics of thin delta wings in the Langley full-scale tunnel, the tests reported herein were made on a 3-percent thick,  $60^\circ$  sweptback delta-wing-fuselage combination with two types of tip controls. These tests included the effects of chord-plane-mounted nacelles at three different spanwise positions on the wing. Aerodynamic forces and moments as well as control hinge-moment data were obtained in the angle-of-attack range of  $-3.7^\circ$  through maximum lift for several control deflections. The test Reynolds number was  $2.3 \times 10^6$  and the Mach number was 0.10.

## COEFFICIENTS AND SYMBOLS

All results are presented in standard NACA form of coefficients of forces and moments. The wing moments are referred to the model axes originating at the projection of the quarter-chord point of the mean aerodynamic chord on the plane of symmetry. The positive directions of forces, moments, and control deflections are shown in figure 1. The coefficients and symbols are defined as follows:

$C_L$  lift coefficient,  $L/qS$

$C_Y$  lateral-force coefficient,  $Y/qS$

$C_m$	pitching-moment coefficient, $M/qS\bar{c}$
$C_n$	yawing-moment coefficient, $N/qSb$
$C_l$	rolling-moment coefficient, $L'/qSb$
$C_h$	hinge-moment coefficient, half-delta tip control, $H/qS_a\bar{c}_a$
$C_h$	hinge-moment coefficient, horn-balanced tip control, $H/2qQ$
$C_{m\delta_r}$	rate of change of pitching-moment coefficient with right control deflection, $\partial C_m/\partial \delta_r$
$C_{l\delta_r}$	rate of change of rolling-moment coefficient with right control deflection, $\partial C_l/\partial \delta_r$
$C_{h\alpha}$	rate of change of hinge-moment coefficient with angle of attack, $\partial C_h/\partial \alpha$
$C_{h\delta_r}$	rate of change of hinge-moment coefficient with right control deflection, $\partial C_h/\partial \delta_r$
$L$	lift, lb
$Y$	lateral force, lb
$M$	pitching moment, ft-lb
$N$	yawing moment, ft-lb
$L'$	rolling moment, ft-lb
$H$	hinge moment, ft-lb
$\rho$	mass density of air, slugs/cu ft
$q$	free-stream dynamic pressure, $\frac{1}{2}\rho V^2$ , lb/sq ft
$V$	free-stream velocity, ft/sec
$S$	total wing area, sq ft
$S_a$	area of one control surface, sq ft
$Q$	moment of area of control surface rearward of hinge line about hinge line, ft <sup>3</sup>

c	wing chord measured parallel to plane of symmetry, ft
$\bar{c}$	wing mean aerodynamic chord measured parallel to plane of symmetry, $\frac{2}{S} \int_0^{b/2} c^2 dy$ , ft
$\bar{c}_a$	control mean aerodynamic chord
b	wing span, ft
y	distance along lateral axis, ft
$\alpha$	angle of attack of wing chord line, deg
$\delta$	control deflection, positive trailing-edge down, deg
$x_o$	longitudinal fuselage and nacelle coordinate, in.
$y_o$	lateral fuselage and nacelle coordinate, in.

Subscripts:

r	right
l	left

#### MODEL AND TESTS

The model of this investigation had a delta-plan-form wing with 60° sweepback at the leading edge, an aspect ratio of 2.31, and NACA 65A003 airfoil sections parallel to free stream. The wing was symmetrically located on the fuselage with the maximum thickness point of the fuselage 0.17 $\bar{c}$  ahead of the 0.25 $\bar{c}$  point on the wing. Coordinates for the fuselage, nacelles, and wing section are given in tables I and II. The general arrangement of the model and controls, as well as the three nacelle positions investigated, are shown in figure 2. The nacelles were tested at three spanwise stations ( $0.33\frac{b}{2}$ ,  $0.48\frac{b}{2}$ , and  $0.67\frac{b}{2}$ ). A more detailed drawing of the controls is given in figure 3. As shown in this figure, the controls were tested in two configurations, a half-delta tip control (configuration A) and a horn-balance-type control (configuration B). The total control areas of the two controls were 5.2 and 10.2 percent of the total wing area, respectively. Illustrations and designations of the configurations tested are shown in figure 4. Six configurations

based on the two types of controls and three nacelle locations were used in the investigation. Both controls were tested without nacelles on the model. In addition, the half-delta tip control was tested with the  $0.48\frac{b}{2}$  and  $0.67\frac{b}{2}$  nacelles and the horn-balance-type control was tested with the  $0.33\frac{b}{2}$  and  $0.48\frac{b}{2}$  nacelles. For most of the tests the controls were deflected on the right wing only, with the exception of some exploratory tests made with the left- and right-wing controls deflected as ailerons ( $\delta_r = -\delta_l$ ).

Aerodynamic forces and moments and hinge-moment data were obtained through the angle-of-attack range of  $-3.7^\circ$  to  $36.3^\circ$  at zero yaw for control deflections of  $-40^\circ$ ,  $-30^\circ$ ,  $-20^\circ$ ,  $-10^\circ$ ,  $0^\circ$ ,  $10^\circ$ ,  $20^\circ$ , and  $30^\circ$ . The data were taken by means of a six-component strain-gage balance in the fuselage and strain-gage beams attached to the control surfaces. The model was mounted on a sting support for tests in the Langley full-scale tunnel as shown in figures 5 and 6. The model tests were conducted separately from those of the semispan wing shown in figure 6. All tests for the delta wing were conducted with the semispan wing set at zero-lift attitude after detailed flow surveys made for this condition did not indicate any interference effects. The tests were made at a Reynolds number of  $2.3 \times 10^6$  based on the mean aerodynamic chord and at a Mach number of 0.10. The data have been corrected for jet blockage and an average stream angle of  $0.3^\circ$ . Calculations were made to determine the jet-boundary correction (by method of ref. 7) and buoyancy correction as applied to the data, but they were found to be negligible and therefore were not applied. The controls were not rigid and the control deflection angles have not been corrected for additional deflection caused by air loads on the surfaces; however, a plot of control deflection due to hinge-moment against hinge-moment coefficient is shown in figure 7. The estimated accuracies of other quantities are:

$\alpha$ , deg . . . . .	$\pm 0.2$
Aerodynamic forces and moments, percent . . . . .	$\pm 2$
Hinge-moment coefficients . . . . .	$\pm 0.008$

#### PRESENTATION OF DATA

The longitudinal characteristics (lift and pitching moment) of the several model configurations tested are presented in figure 8. In order to isolate the effects of the nacelles on the longitudinal control characteristics, the variation of  $C_m$  with  $\delta_r$  for each nacelle-control configuration is presented in figure 9. Longitudinal control effectiveness ( $C_{m\delta_r}$  against  $\alpha$  at  $\delta_r = 0^\circ$ ) is given in figure 10. Figure 11

shows a comparison of the total rolling-moment coefficients for control deflections of  $\delta_r = 20^\circ$  and  $\delta_l = -20^\circ$  with the equivalent total rolling-moment coefficients as obtained by combining the rolling moments produced by the right wing control only at  $\delta_r = 20^\circ$  and  $-20^\circ$ . The basic lateral characteristics ( $C_y$ ,  $C_n$ , and  $C_l$  against  $\alpha$  for each control configuration) are presented in figure 12, and control effectiveness data ( $C_l$  against  $\delta_r$ ) are shown in figure 13. In figure 14 the variation of the control parameter  $C_{l\delta_r}$  with angle of attack at  $\delta_r = 0^\circ$ ,  $-10^\circ$ , and  $-20^\circ$  is given for both control configurations with and without nacelles. The variations of yawing-moment coefficient with control deflection at several angles of attack are given in figure 15. The hinge-moment characteristics ( $C_h$  against  $\alpha$  and  $C_h$  against  $\delta_r$ ) for all the control configurations are shown in figures 16 and 17, respectively.

## RESULTS

### Longitudinal Characteristics

The lift and static longitudinal stability characteristics of the basic model without controls for several nacelle installations on the wing have been presented in reference 6. Although the main purpose of the present tests is to determine the lateral control characteristics of the various model-control combinations, there is current interest in using trailing-edge controls as longitudinal as well as lateral control devices; therefore, a brief discussion of the longitudinal control characteristics as obtained from single control tests is presented here.

As can be seen from figure 10 the longitudinal-control capabilities of the half-delta tip control on the basic model without nacelles are small ( $C_{m\delta_r} = -0.00089$  at  $\delta_r = 0^\circ$  and  $\alpha = 0.3^\circ$ ). This result would be expected since the control area is only approximately 5 percent of the semispan-wing area and the moment arm of the control hinge line about the arbitrary model center of gravity (0.25c) is only 58 percent of the mean aerodynamic chord. The horn-balance-type control is approximately twice as effective as a longitudinal control as the half-delta tip control ( $C_{m\delta_r} = -0.002$  at  $\delta_r = 0^\circ$  and  $\alpha = 0.3^\circ$ ). Control effectiveness of both controls decreased with increasing angle of attack,  $C_{m\delta_r}$  equaling approximately  $-0.0006$  and  $-0.0012$  at  $\alpha = 24.3^\circ$  for the half-delta and horn-balance-type controls, respectively. Addition of the inboard nacelles to the half-delta and horn-balance-type control configurations (configurations A-48 and B-33) had little effect on the

longitudinal characteristics in the angle-of-attack range presented. The outboard nacelles, (configurations A-67 and B-48) which were adjacent to the half-delta and horn-balance-type controls produced some increases in longitudinal control effectiveness of both types of controls in the low positive to high negative control-deflection range (fig. 9). At  $\alpha = 24.3^\circ$ , the value of  $C_{m\delta_r}$  for the half-delta control with the outboard nacelle increased to -0.00107 and the value of  $C_{m\delta_r}$  for the horn-balance-type control was increased to -0.00145 by its adjacent nacelle.

### Lateral Characteristics

The results of tests made to determine the validity of the assumption that the effectiveness of differentially deflected tip controls would be adequately represented by tests of the control on one semispan are shown in figure 11. Good agreement is indicated up to  $\alpha = 24.3^\circ$  and thus indicated that there was no mutual interference of the semispan loadings due to tip control deflection. The basic lateral-control data ( $C_y$ ,  $C_n$ ,  $C_l$  against  $\alpha$ ) are, therefore, presented for the right semispan control deflected only (fig. 12). From figures 12(a) and 12(d), the rolling-moment characteristics show that control reversals are encountered with positive deflection of the half-delta tip and horn-balance-type controls on the model without nacelles at angles of attack above approximately  $28^\circ$ . This result is probably due to the control stall and its effect on the loading on the outer part of the right wing at these angles of attack which causes an early stall on that semispan. With the nacelles installed the control reversals are alleviated, probably because the nacelles tend to reduce the interaction between the loading on the outboard portion and the inboard portion of the semispan. (See ref. 6.)

In figure 13 ( $C_l$  against  $\delta_r$ ) the lateral control effectiveness of the control configurations exhibited approximately linear characteristics from low positive to moderate negative control deflections through most of the angle-of-attack range, but at positive control deflections greater than  $\delta_r = 10^\circ$  there was a loss in control effectiveness at moderate angles of attack which indicated that the controls had stalled.

The parameter  $C_{l\delta_r}$  for all control configurations (fig. 14) was obtained from figure 13 by taking the approximate slopes of the curve for  $C_l$  against  $\delta_r$  at  $\delta_r = 0^\circ$ ,  $-10^\circ$ , and  $-20^\circ$ . At  $\delta_r = 0^\circ$ , the control effectiveness of the half-delta tip control on the model without nacelles decreased with increasing angle of attack from -0.00055 at



$\alpha = 0.3^\circ$  to  $-0.0003$  at  $\alpha = 28^\circ$ . The horn-balance-type control is twice as effective as the half-delta tip control through most of the angle-of-attack range. This increased effectiveness is more than would be expected by doubling the area of the half-delta tip control (see ref. 4) and can be attributed to the more effectively loaded inboard half of the horn-balance-type control. Addition of the inboard  $\left(0.48\frac{b}{2}\right)$  and  $0.33\frac{b}{2}$  nacelles to the half-delta and horn-balance-type control configurations, respectively, did not generally affect the control effectiveness of the two controls. When the nacelles were moved to positions adjacent to the controls, however, control effectiveness was increased at all angles of attack, especially that of the half-delta tip control. With the adjacent  $\left(0.67\frac{b}{2}\right)$  nacelles installed, the half-delta control maintained constant effectiveness ( $C_{l\delta_r}$  approximately  $-0.0006$ ) up to  $\alpha = 24^\circ$ . The nacelle of this configuration increased the effectiveness of the half-delta tip control more than might be expected on the basis of previous tests of a half-delta tip control with adjacent circular end plates (ref. 4).

The values of  $C_{l\delta_r}$  at  $\delta_r = -10^\circ$  and  $-20^\circ$  indicate that, at angles of attack below  $12^\circ$ , the half-delta and horn-balance-type controls with an initial deflection of  $-10^\circ$  or  $-20^\circ$  would be less effective than the same control with an initial deflection of  $0^\circ$ . Above  $\alpha = 12^\circ$ , there are only small differences in control effectiveness between  $\delta_r = 0^\circ$ ,  $-10^\circ$ , and  $-20^\circ$ . The yawing characteristics introduced by deflecting the controls ( $C_n$  against  $\delta_r$ ) are shown in figure 15. Adverse yawing moments were produced by positive control deflections for all the control configurations tested. The yawing moments of the basic model with negative deflection of the half-delta tip control were favorable through most of the angle-of-attack range. Above  $\alpha = 24.3^\circ$ , however, negative control deflections produced adverse yawing moments. The yawing moments of the basic model with the horn-balance-type control tended to become adverse with small negative control deflections at angles of attack above  $8.3^\circ$ . Addition of the inboard  $\left(0.48\frac{b}{2}\right)$  and  $0.33\frac{b}{2}$  nacelles to the half-delta and horn-balance-type control configurations, respectively, had only small effects on the yawing moments due to control deflection through most of the angle-of-attack range; however, at high angles of attack (above  $\alpha = 24.3^\circ$ ), they tended to reduce the adverse yawing moments of the basic model at negative control deflections. With the outboard  $\left(0.67\frac{b}{2}\right)$  nacelles installed on the half-delta control configuration, negative deflection of the control produced large adverse yawing moments, especially at high angles of attack. Near maximum lift,

control deflections of  $-20^\circ$  to  $-30^\circ$  produced an adverse yawing-moment coefficient of approximately  $-0.012$ . The outboard  $\left(0.48\frac{b}{2}\right)$  nacelles had little effect on the yawing characteristics of the horn-balance-type control configuration.

### Hinge-Moment Characteristics

The hinge-moment characteristics of the half-delta-tip and horn-balance-type control configurations are given in figures 16 and 17. As can be seen in figure 16(a) there is generally a positive value of  $C_{h\alpha}$  in the low angle-of-attack range ( $\alpha = 0.3^\circ$  to  $4.3^\circ$ ) for all the half-delta tip-control configurations. At these low angles of attack, the control is virtually balanced as shown in figure 17(a). Above  $\alpha = 4.3^\circ$ , the control on the model without nacelles exhibited increasingly nonlinear hinge-moment characteristics, and  $C_{h\alpha}$  tended to become negative (fig. 16(a)). In either case the hinge moments are small and, as the control is nearly balanced, it is subject to erratic hinge-moment characteristics, even with small center-of-pressure variations which are known to occur on the tips of delta wings having the leading-edge separation vortex passing across the control at moderate angles of attack. Addition of the inboard  $\left(0.48\frac{b}{2}\right)$  nacelles to the half-delta control configuration (fig. 17(a)) produced only minor changes in the hinge-moment characteristics of the control; however, the outboard  $\left(0.67\frac{b}{2}\right)$  nacelles caused considerable change in the hinge moments at negative control deflections for all angles of attack above  $4^\circ$ . At these angles the nacelles caused the controls to exhibit increasingly positive hinge moments at negative control deflections, this positive increment in  $C_h$  being equal to approximately  $0.12$  at  $\alpha = 20.3^\circ$  and  $\delta_r = -20^\circ$ .

The hinge-moment characteristics of the horn-balance-type control on the model without nacelles (figs. 16(b) and 17(b)) were similar to those of an outboard trailing-edge control as shown by previous tests on the 10-percent-thick  $60^\circ$  delta wing with trailing-edge controls and having leading-edge-separation vortex-type flow (ref. 8). This result might be expected since the horn-balance-type control is essentially a trailing-edge type of control with a horn-balance having only 12 percent of the control-surface area and the control is subjected to similar wing-flow characteristics. The control has large negative values of  $C_{h\alpha}$  and  $C_{h\delta_r}$  through most of the angle-of-attack range, some nonlinear characteristics occurring at high angles of attack and large control deflections. Addition of the nacelles (figs. 16(c) and 16(d))

causes a reduction in the slope of the curve for  $C_h$  against  $\alpha$  especially at the higher angles of attack; this reduction indicates a forward shift of the control center of pressure resulting from the influence of the nacelles on the basic flow characteristics over the outboard section of the wing. (See ref. 6.) The nacelles had little effect on the variation of  $C_h$  with  $\delta_r$  for the horn-balance-type control at low angles of attack; however, at angles of attack above  $12^\circ$ , the nacelles tend to reduce  $C_{h\delta_r}$  at positive control deflections (fig. 17(b)). In addition, the outboard ( $0.48\frac{b}{2}$ ) nacelles increased  $C_{h\delta_r}$  at negative control deflections in the same angle-of-attack range.

#### SUMMARY OF RESULTS

The results of the low-speed investigation of the aerodynamic, control, and hinge-moment characteristics of a delta-wing-fuselage model with half-delta tip controls and horn-balance-type controls of 5.2 and 10.2 percent of the total wing area, respectively, with and without chord-plane-mounted nacelles may be summarized as follows:

1. The half-delta tip control on the model without nacelles had low longitudinal and lateral control effectiveness in the higher angle-of-attack range. The horn-balance-type control on the model without nacelles had about twice the longitudinal and lateral control effectiveness of the half-delta tip control through most of the angle-of-attack range.

2. Both controls on the model without nacelles produced adverse yawing characteristics at positive control deflections throughout the angle-of-attack range. At the higher angles of attack, negative deflection of both controls also produced adverse yawing characteristics.

3. The presence of the inboard ( $0.48$  semispan and  $0.33$  semispan) nacelles had only minor effects on the longitudinal and lateral control effectiveness of the half-delta and horn-balance-type controls, respectively, but the adjacent nacelles ( $0.67$  semispan and  $0.48$  semispan, respectively) increased the longitudinal and lateral control effectiveness of both controls, especially the half-delta tip control.

4. The inboard ( $0.33$  semispan and  $0.48$  semispan) nacelles did not have much effect on the yawing characteristics due to control deflection of the half-delta and horn-balance-type controls, respectively. The outboard ( $0.67$  semispan) nacelles on the model with the half-delta tip control caused large adverse yawing moments at negative control deflections and angles of attack above  $12.3^\circ$ .

5. The half-delta tip control exhibited nonlinear hinge-moment characteristics, although the hinge moments were small because the control was nearly balanced. The horn-balance-type control hinge moments varied more nearly linear with control deflection and angle of attack and were characterized by high negative values of the rate of change of hinge-moment coefficient with angle of attack and right control deflection ( $C_{h\alpha}$  and  $C_{h\delta_r}$ ) and large hinge moments.

6. The 0.67 semispan nacelles caused a large positive increment in hinge-moment coefficients of the half-delta tip control at negative control deflections and angles of attack above 4.3. The 0.48 semispan nacelle on the half-delta tip-control configuration and the 0.33 semispan and 0.48 semispan nacelle locations on the horn-balance-type control configuration had only small effects on the basic hinge-moment characteristics of the half-delta and horn-balance-type controls, respectively.

Langley Aeronautical Laboratory,  
National Advisory Committee for Aeronautics,  
Langley Field, Va.

## REFERENCES

1. Sandahl, Carl A., and Strass, H. Kurt: Comparative Tests of the Rolling Effectiveness of Constant-Chord, Full-Delta, and Half-Delta Ailerons on Delta Wings at Transonic and Supersonic Speeds. NACA RM L9J26, 1949.
2. Thomas, G. B.: Analysis of Additional Supersonic Wind-Tunnel Tests of Balanced Aileron Configurations for the Nike Guided Missile. Rep. No. SM-14290, Douglas Aircraft Co., Inc., Mar. 14, 1952.
3. Martz, C. William, Church, James D., and Goslee, John W.: Rocket-Model Investigation To Determine the Force and Hinge-Moment Characteristics of a Half-Delta Tip Control on a  $59^\circ$  Sweptback Delta Wing Between Mach Numbers of 0.55 and 1.43. NACA RM L52H06, 1952.
4. Jaquet, Byron M., and Queijo, M. J.: Low-Speed Wind-Tunnel Investigation of Lateral Control Characteristics of a  $60^\circ$  Triangular-Wing Model Having Half-Delta Tip Controls. NACA RM L51I10, 1951.
5. Lichtenstein, Jacob H., and Jaquet, Byron M.: Low-Speed Static Longitudinal Stability and Control Characteristics of  $60^\circ$  Triangular- and Modified  $60^\circ$  Triangular-Wing Models Having Half-Delta and Half-Diamond Tip Controls. NACA RM L51K08, 1952.
6. Scallion, William I.: Low-Speed Investigation of the Effects of Nacelles on the Longitudinal Aerodynamic Characteristics of a  $60^\circ$  Sweptback Delta-Wing—Fuselage Combination With NACA 65A003 Airfoil Sections. NACA RM L52F04, 1952.
7. Katzoff, S., and Hannah, Margery E.: Calculation of Tunnel-Induced Upwash Velocities for Swept and Yawed Wings. NACA TN 1748, 1948.
8. Hawes, John G., and May, Ralph W., Jr.: Investigation at Low Speed of the Effectiveness and Hinge Moments of a Constant-Chord Ailavator on a Large-Scale Triangular Wing With Section Modification. NACA RM L51A26, 1951.

TABLE I

## COORDINATES OF FUSELAGE AND NACELLES

## Fuselage ordinates

Station	$x_0$ , in.	$y_0$ , in.
0	0	0
1	.72	.333
2	1.08	.4284
3	1.80	.6156
4	3.60	1.040
5	7.20	1.735
6	10.80	2.322
7	14.40	2.838
8	21.60	3.733
9	28.80	4.449
10	36.00	4.989
11	43.20	5.387
12	50.40	5.662
13	57.60	5.850
14	64.80	5.965
15	72.00	6.001
16	79.20	5.947
17	86.40	5.794
18	93.60	5.466
19	100.80	5.128
20	108.00	4.789
21	115.20	4.453
22	120.00	4.224
Nose radius = 0.072 in.		

## Nacelle ordinates

Station	$x_0$ , in.	$y_0$ , in.
0	0	0
1	.279	.195
2	.921	.471
3	2.315	.937
4	3.170	1.364
5	5.106	1.735
6	6.500	2.084
7	7.198	2.232
8	8.252	2.444
9	10.002	2.717
10	13.503	3.083
11	17.005	3.320
12	20.51	3.459
13	24.00	3.501
14	46.95	3.501
15	49.86	3.451
16	52.77	3.334
17	55.67	3.144
18	58.58	2.871
19	61.48	2.536
20	64.39	2.142
21	67.29	1.719
22	67.65	1.668
Nose radius = 0.139 in.		

NACA

TABLE II

## NACA 65A003 AIRFOIL ORDINATES

Station, percent chord	y, percent chord
0	0
.5	.234
.75	.284
1.25	.362
2.50	.493
5.00	.658
7.50	.796
10.00	.912
15.00	1.097
20.00	1.236
25.00	1.342
30.00	1.420
35.00	1.472
40.00	1.498
45.00	1.497
50.00	1.465
55.00	1.402
60.00	1.309
65.00	1.191
70.00	1.053
75.00	.897
80.00	.727
85.00	.549
90.00	.369
95.00	.188
100.00	.007
L. E. radius = 0.058% <i>c</i>	

NACA

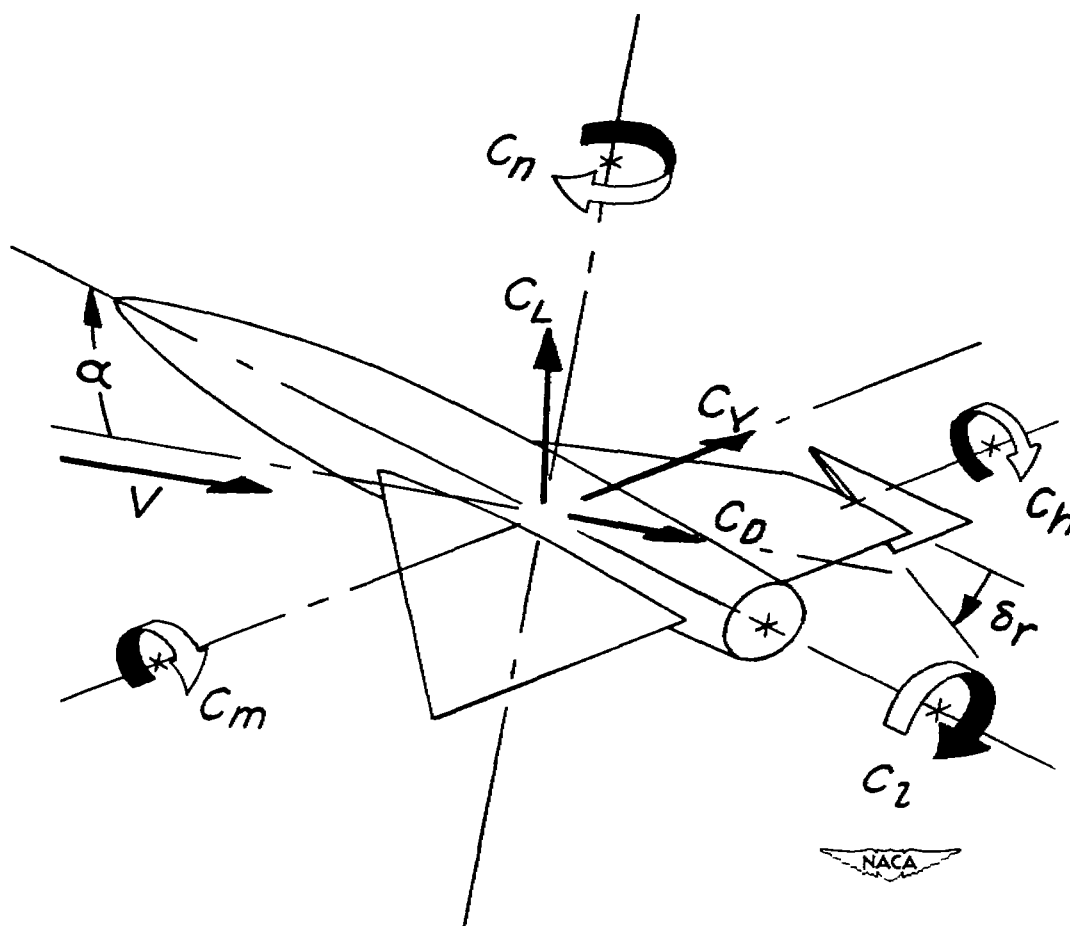


Figure 1.- System of axes used. Arrows indicate positive direction of forces, moments, and angular displacements.



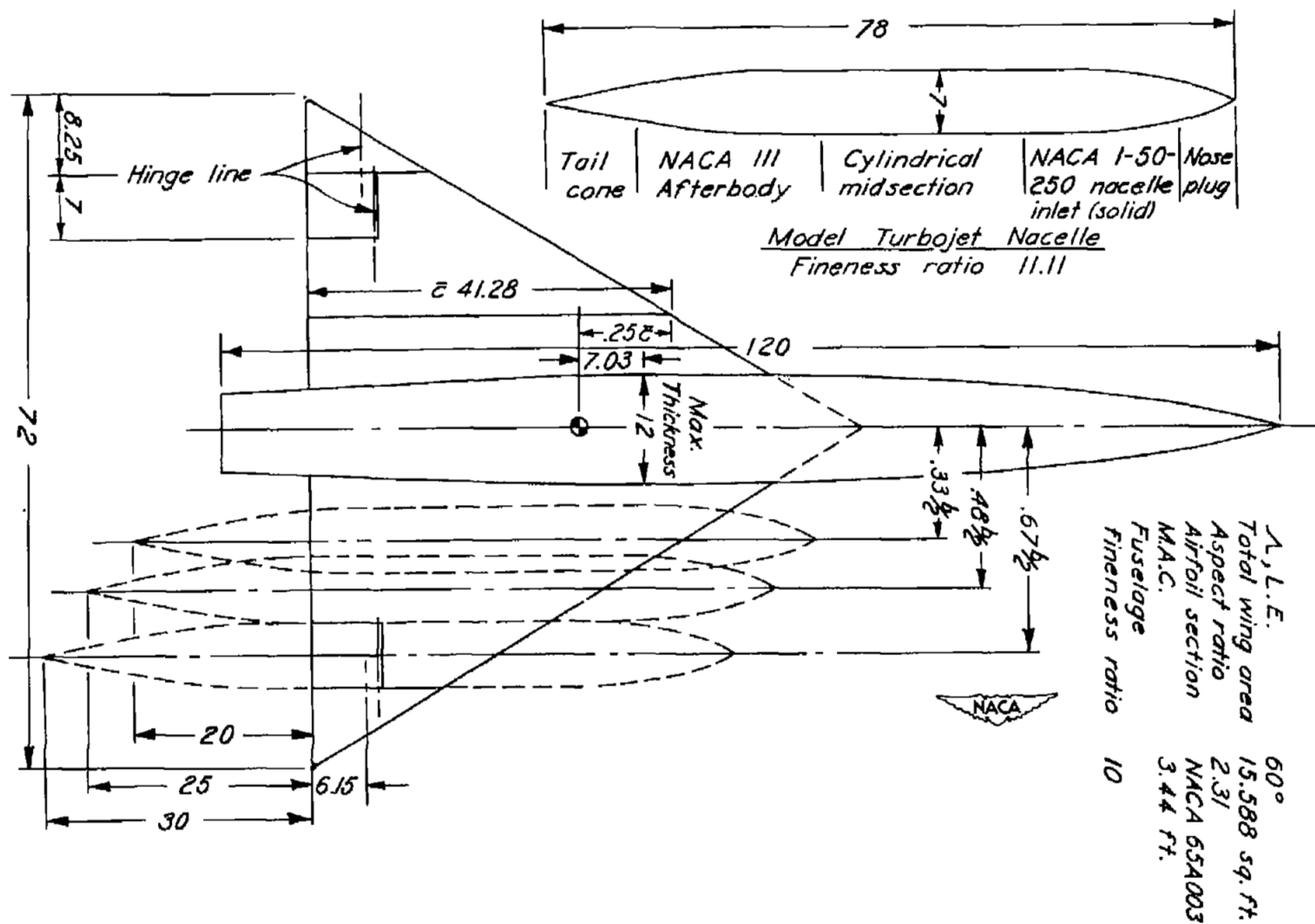
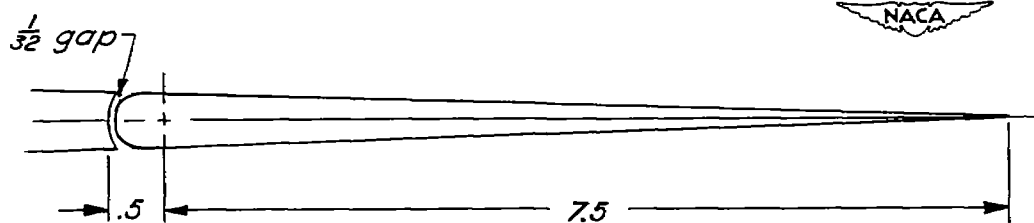
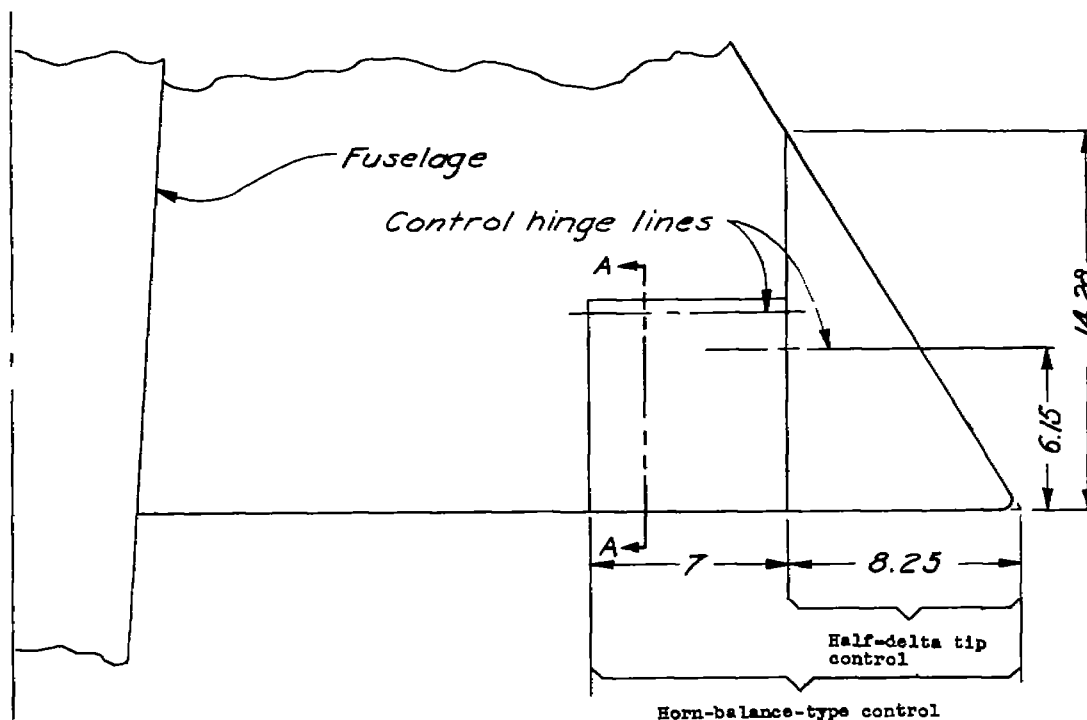


Figure 2.- General arrangement and principal dimensions of the 60° delta-wing model. All dimensions are given in inches.

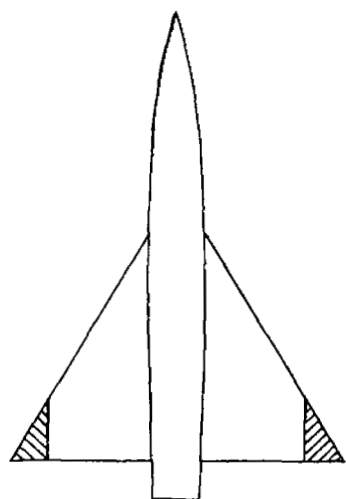


### Section A-A

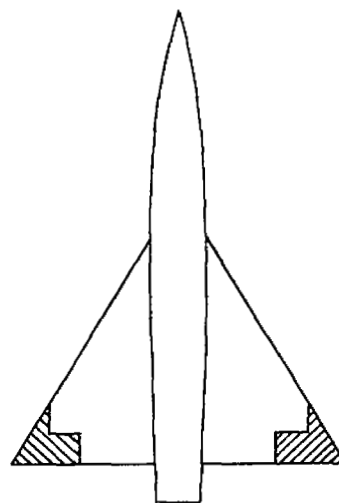
#### Model Control Details

	Half-delta tip control	Horn- balanced tip control
Total control area, both wings	0.81 sq ft	1.59 sq ft
<u>Total control area</u> <u>Total wing area</u>	0.052	0.102
Hinge-line location	0.57 control root chord	0.88 wing root chord
Inboard end of control	0.77 b/2	0.576 b/2
Outboard end of control	1.00 b/2	1.00 b/2

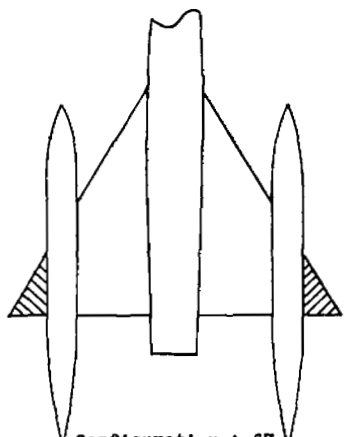
Figure 3.- Details of the model control surfaces. All dimensions are given in inches.



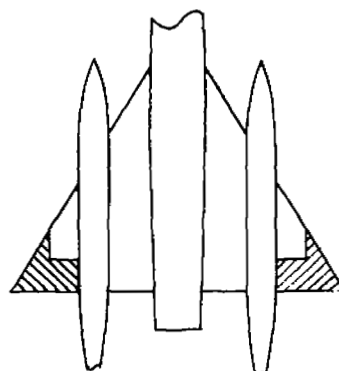
Configuration A  
Half-delta tip controls



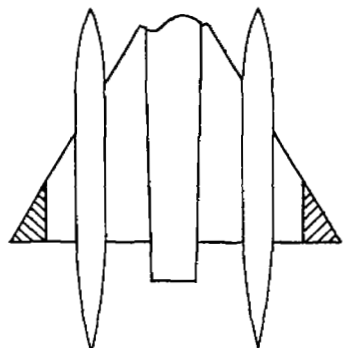
Configuration B  
Horn-balance-type controls



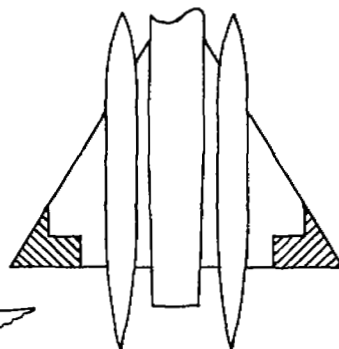
Configuration A-67  
Half-delta tip controls  
and 0.67b/2 nacelles



Configuration B-48  
Horn-balance-type controls  
and 0.48b/2 nacelles



Configuration A-48  
Half-delta tip controls  
and 0.48b/2 nacelles



Configuration B-33  
Horn-balance-type controls  
and 0.33b/2 nacelles

Figure 4.- Arrangement of control and nacelle configurations tested.

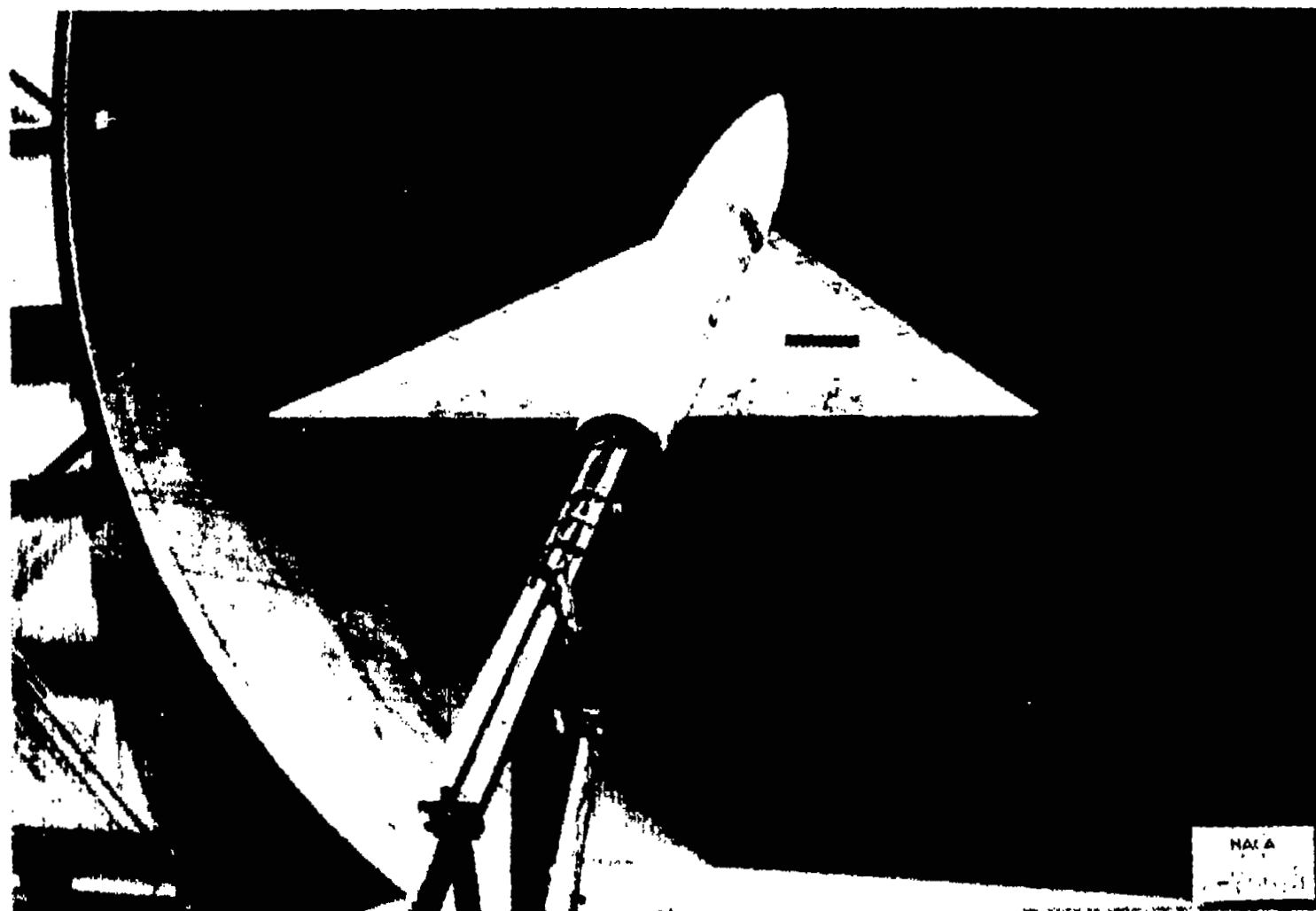


Figure 5.- Photograph of the  $60^\circ$  delta-wing model without nacelles as mounted in the Langley full-scale tunnel.

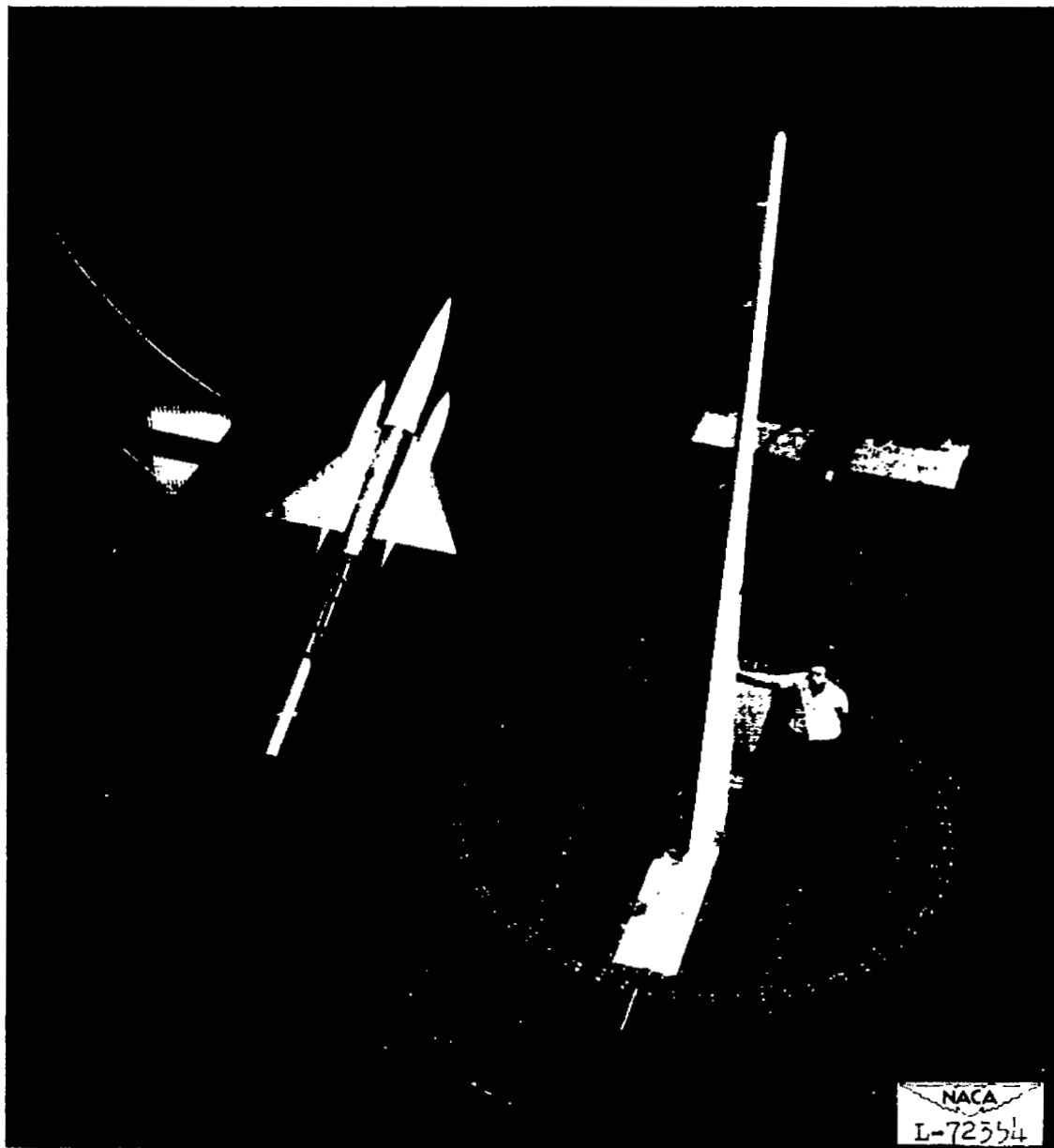


Figure 6.- General view of the  $60^\circ$  delta-wing model with nacelles mounted in the Langley full-scale tunnel.

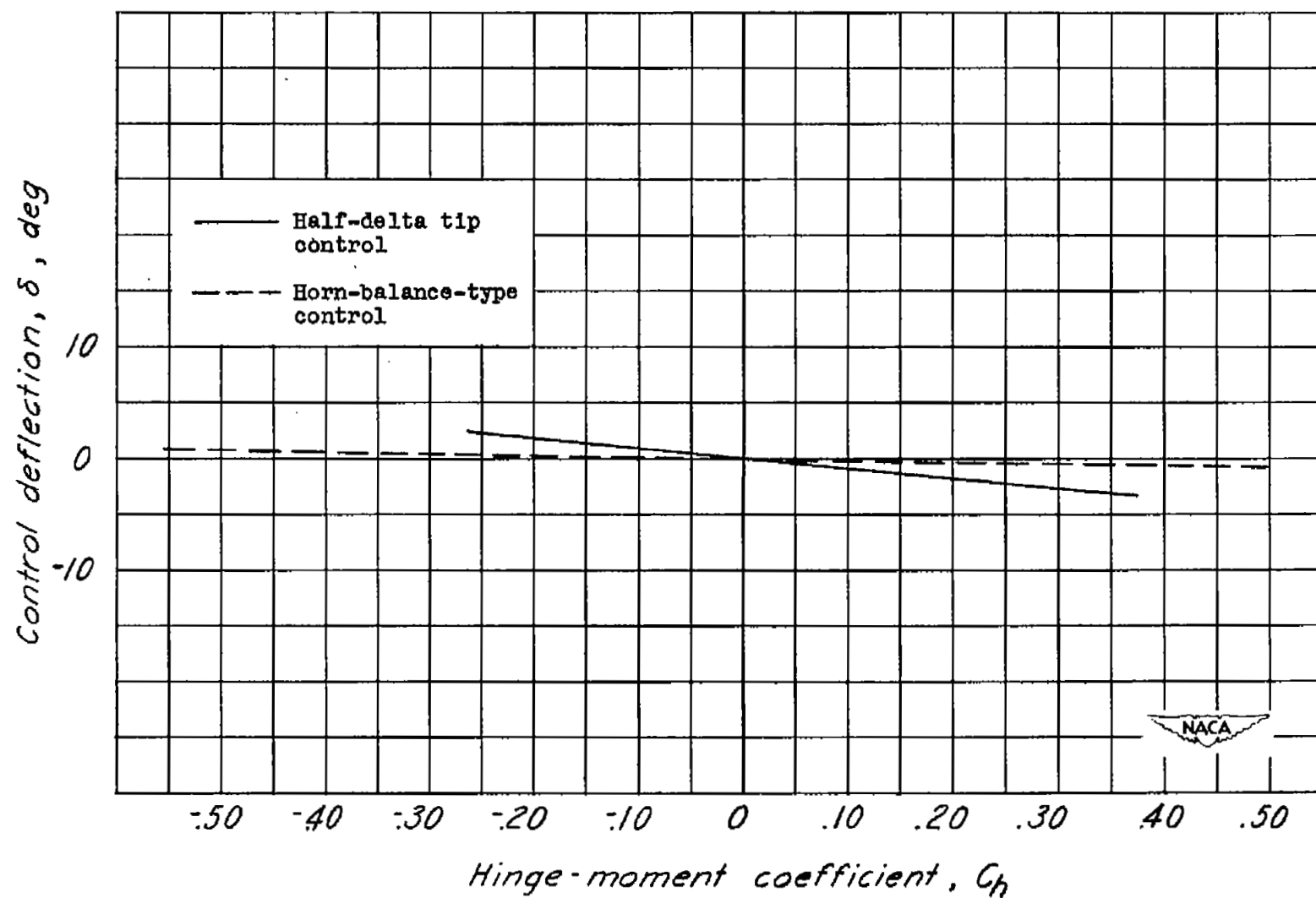
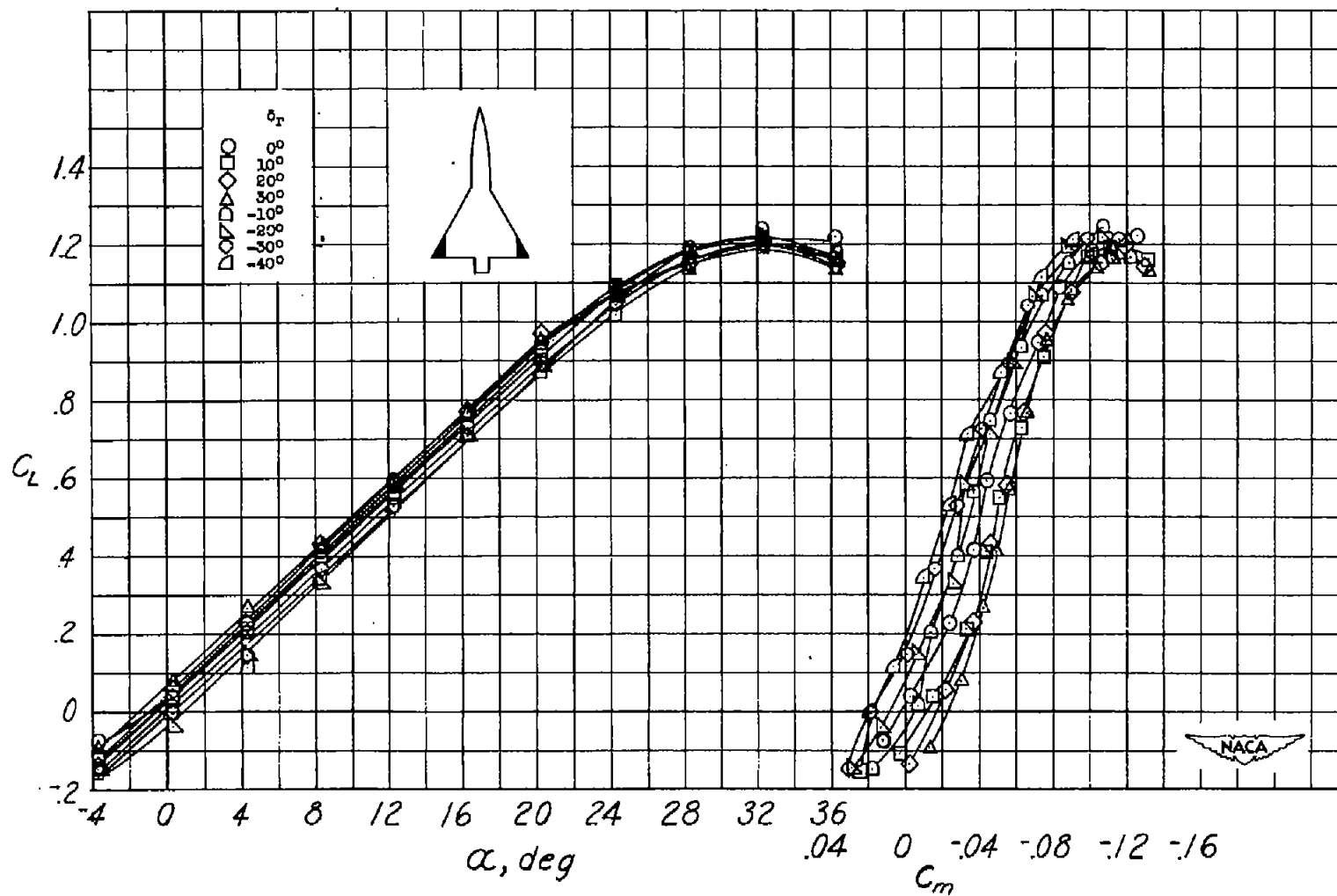
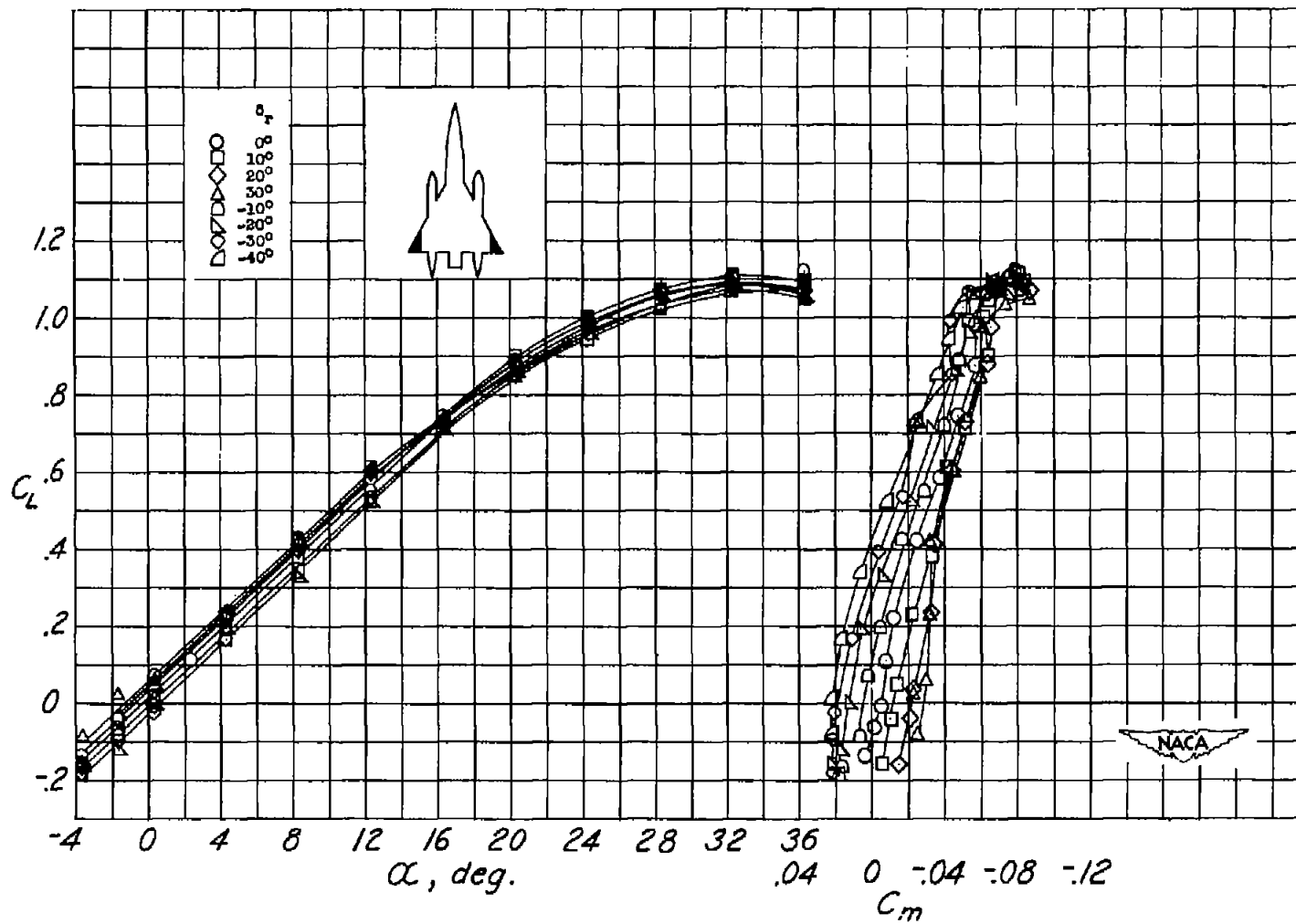


Figure 7.- Deflection of control surfaces due to load.



(a) Configuration A.

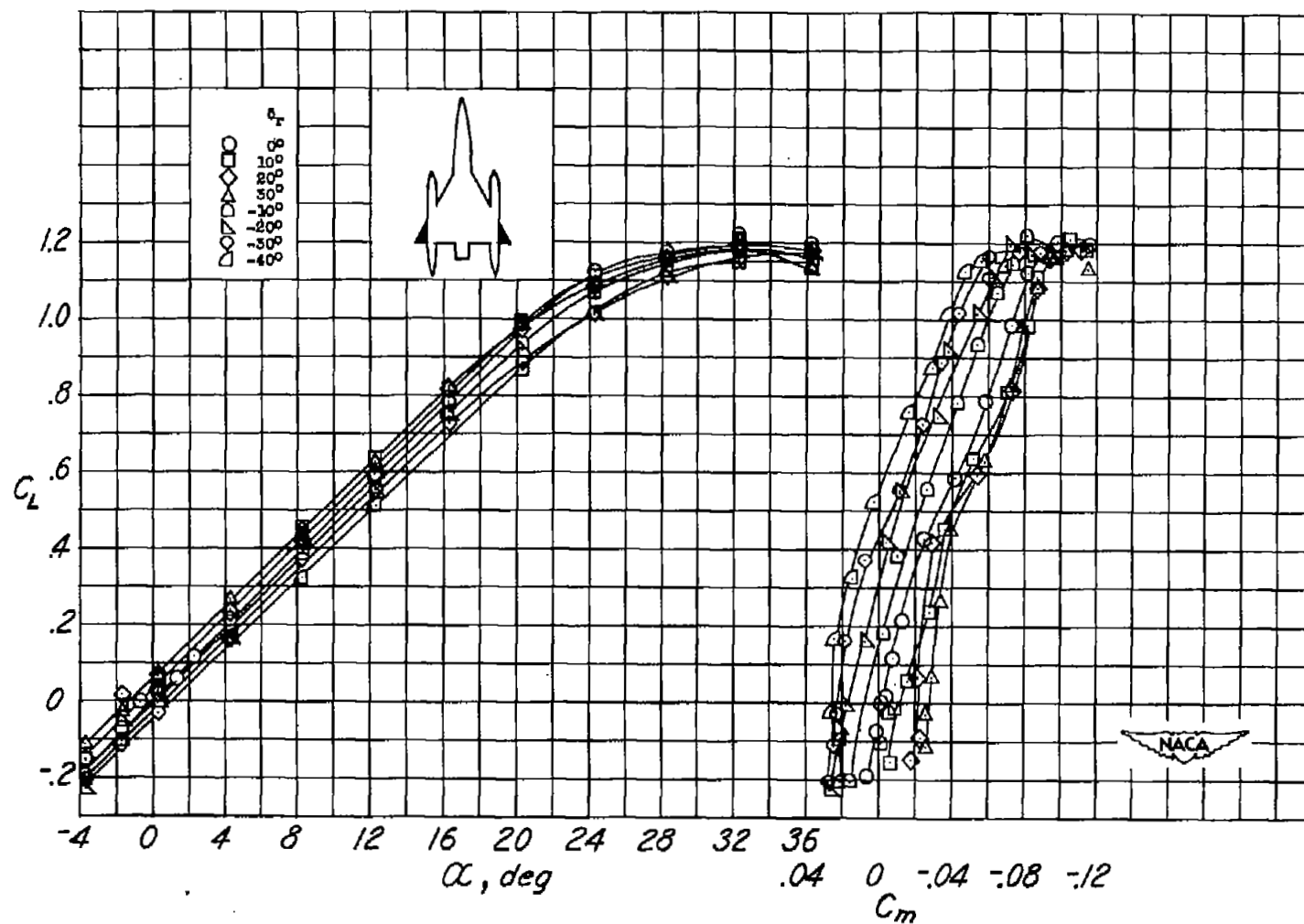
Figure 8.- Longitudinal characteristics of the delta-wing model.



(b) Configuration A-48.

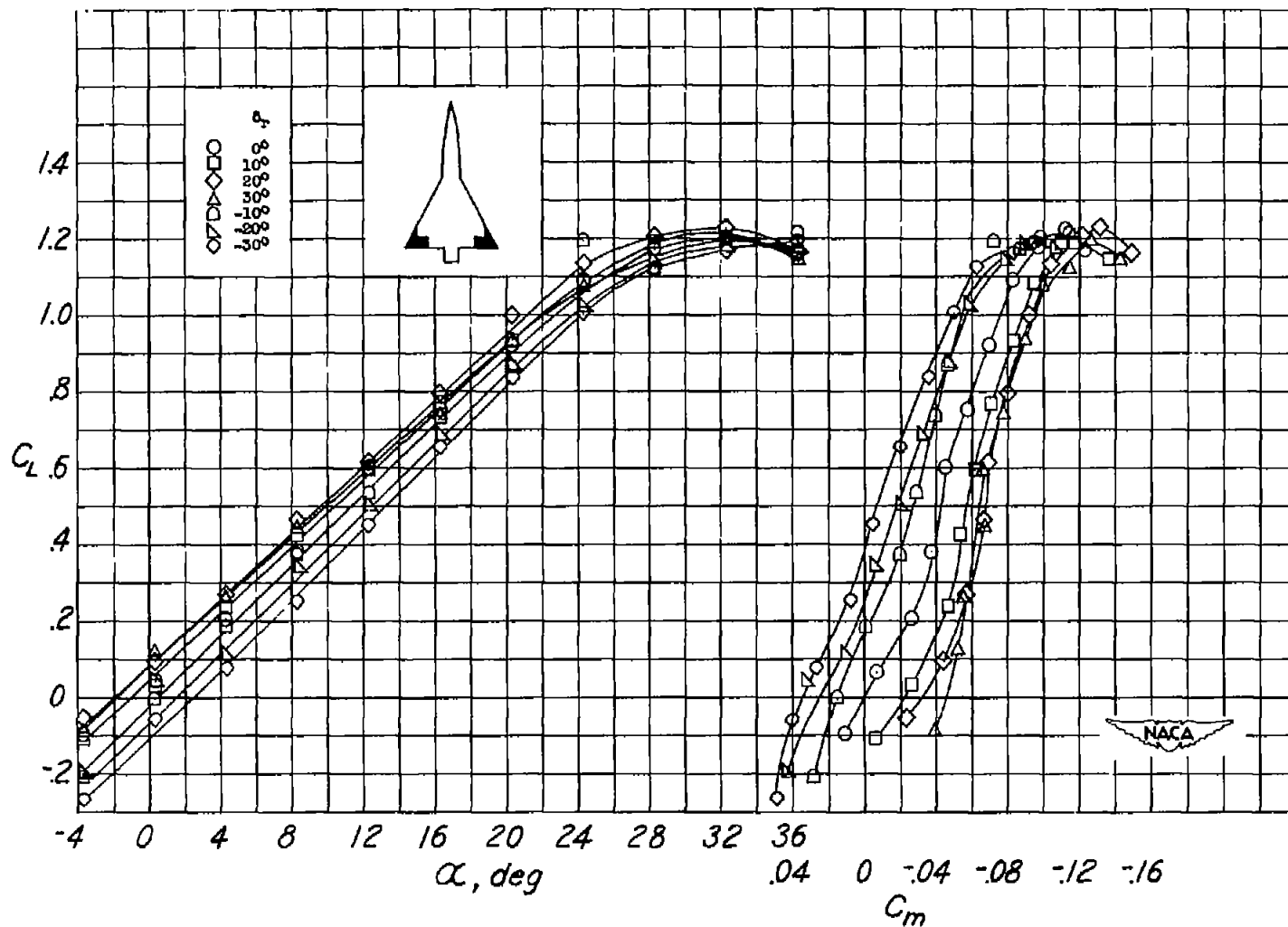
Figure 8.- Continued.

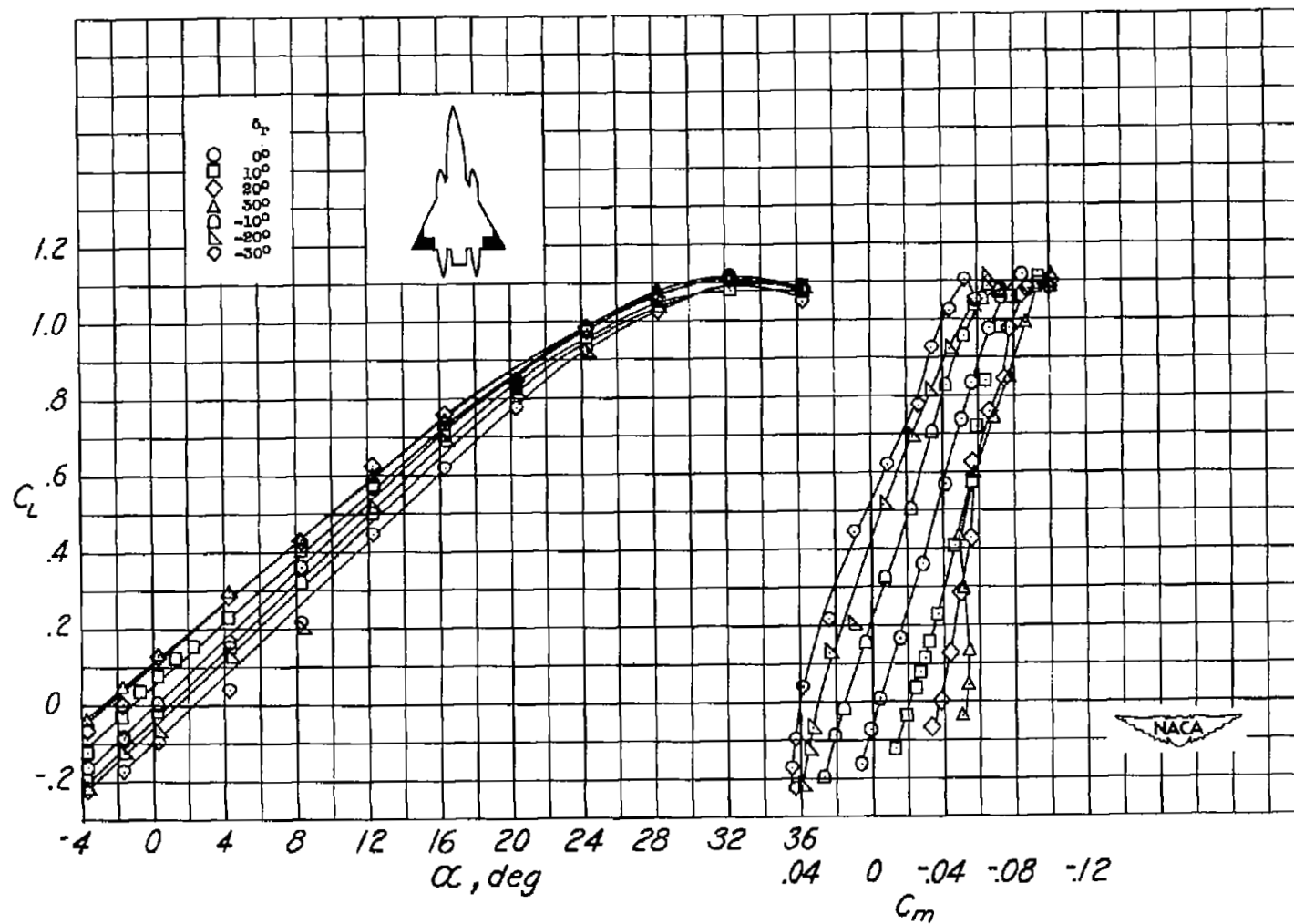




(c) Configuration A-67.

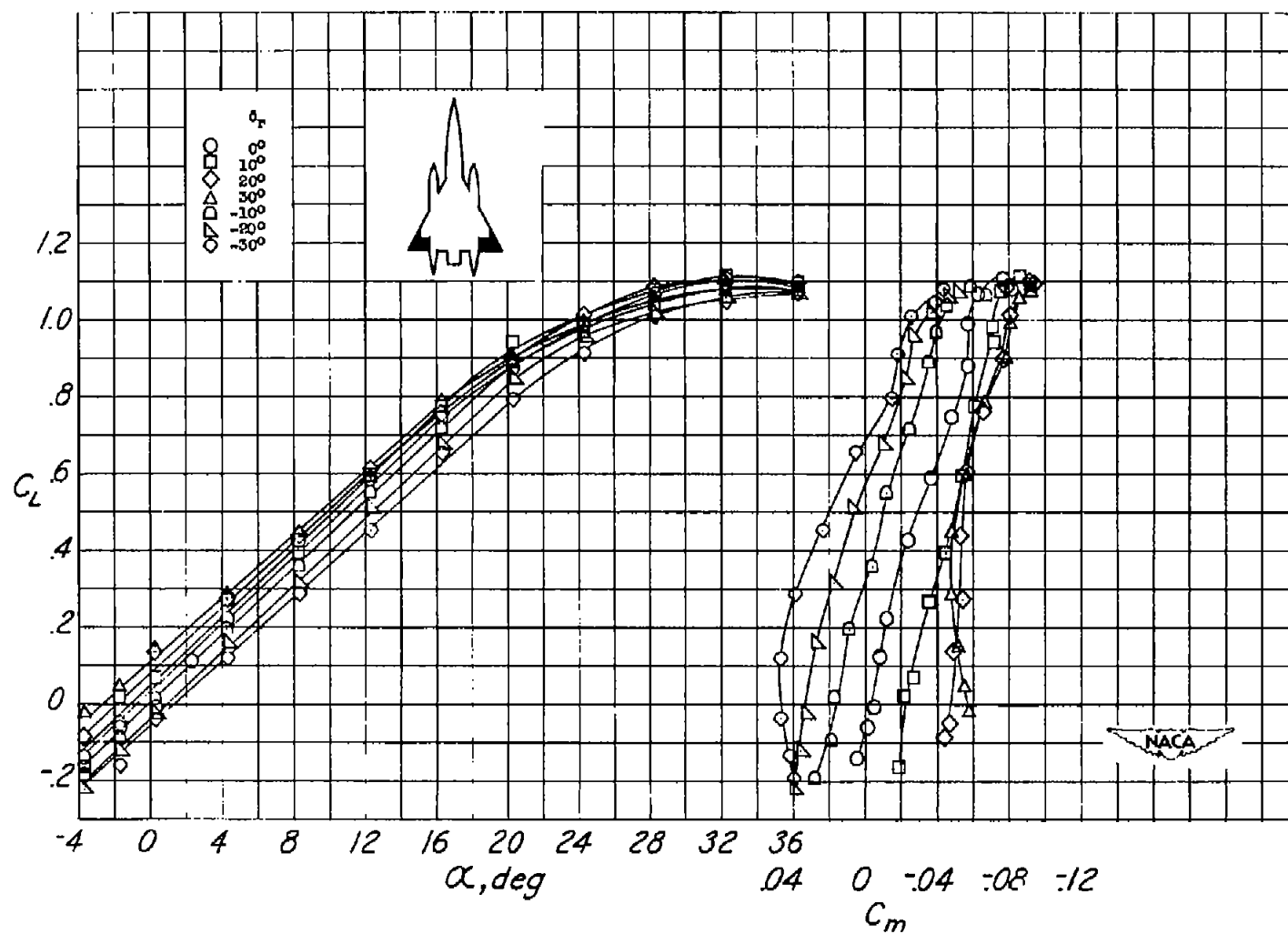
Figure 8.- Continued.





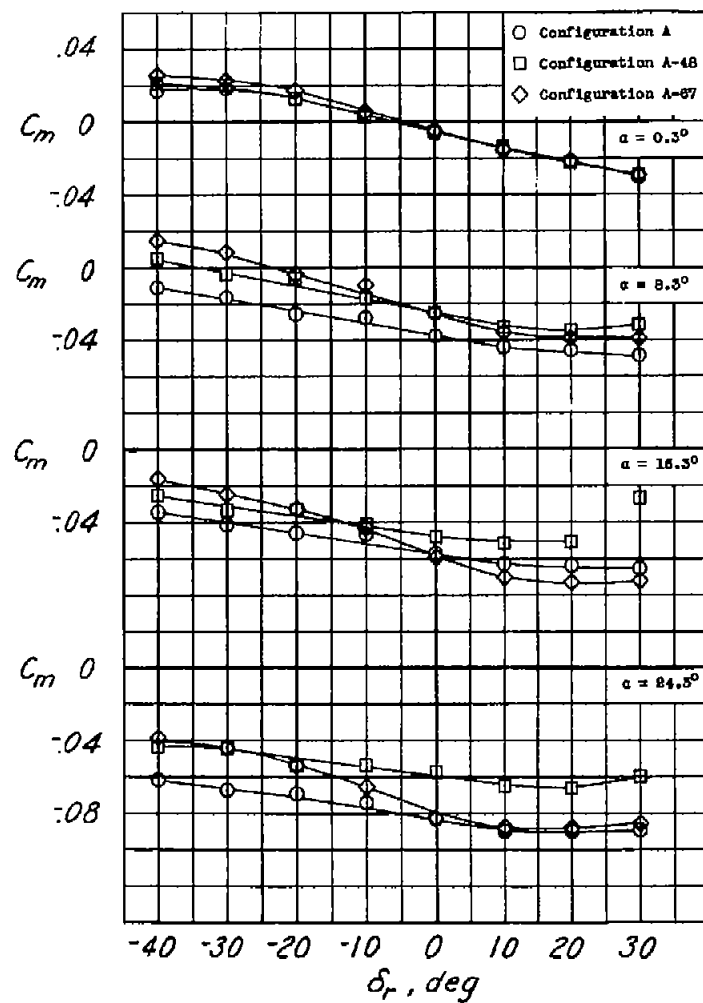
(e) Configuration B-33.

Figure 8.- Continued.

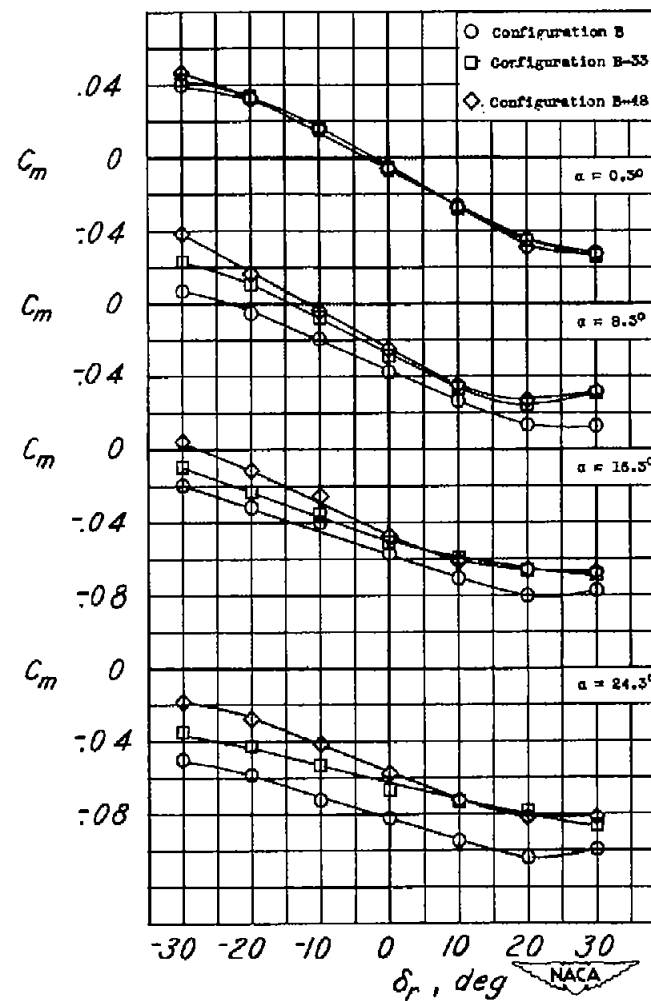


(f) Configuration B-48.

Figure 8.- Concluded.



(a) Half-delta tip control.



(b) Horn-balance-type control.

Figure 9.- Variation of pitching-moment coefficient with control deflection.

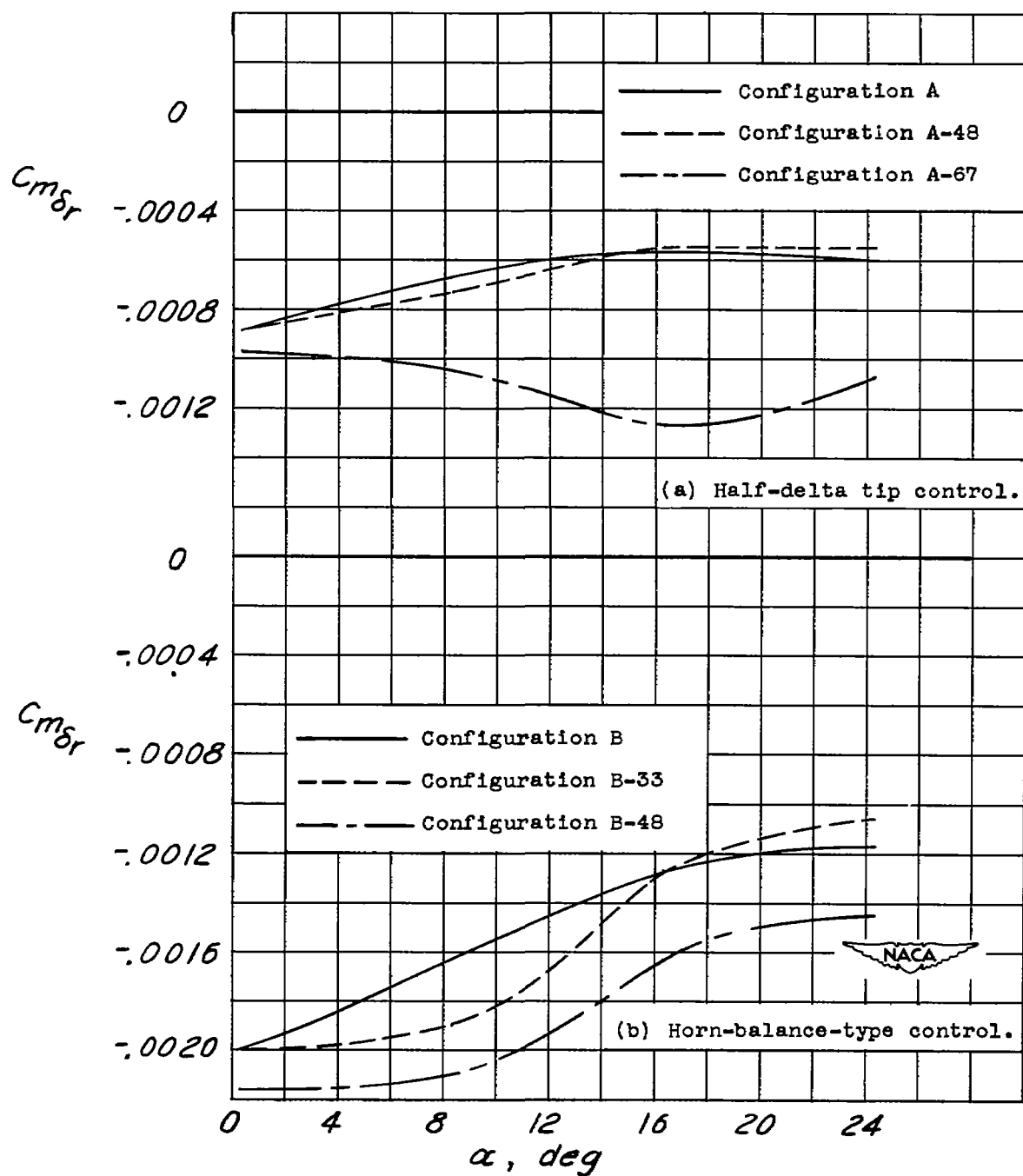


Figure 10.- Variation of  $C_{m\delta_r}$  with angle of attack ( $\delta_r = 0^\circ$ ).

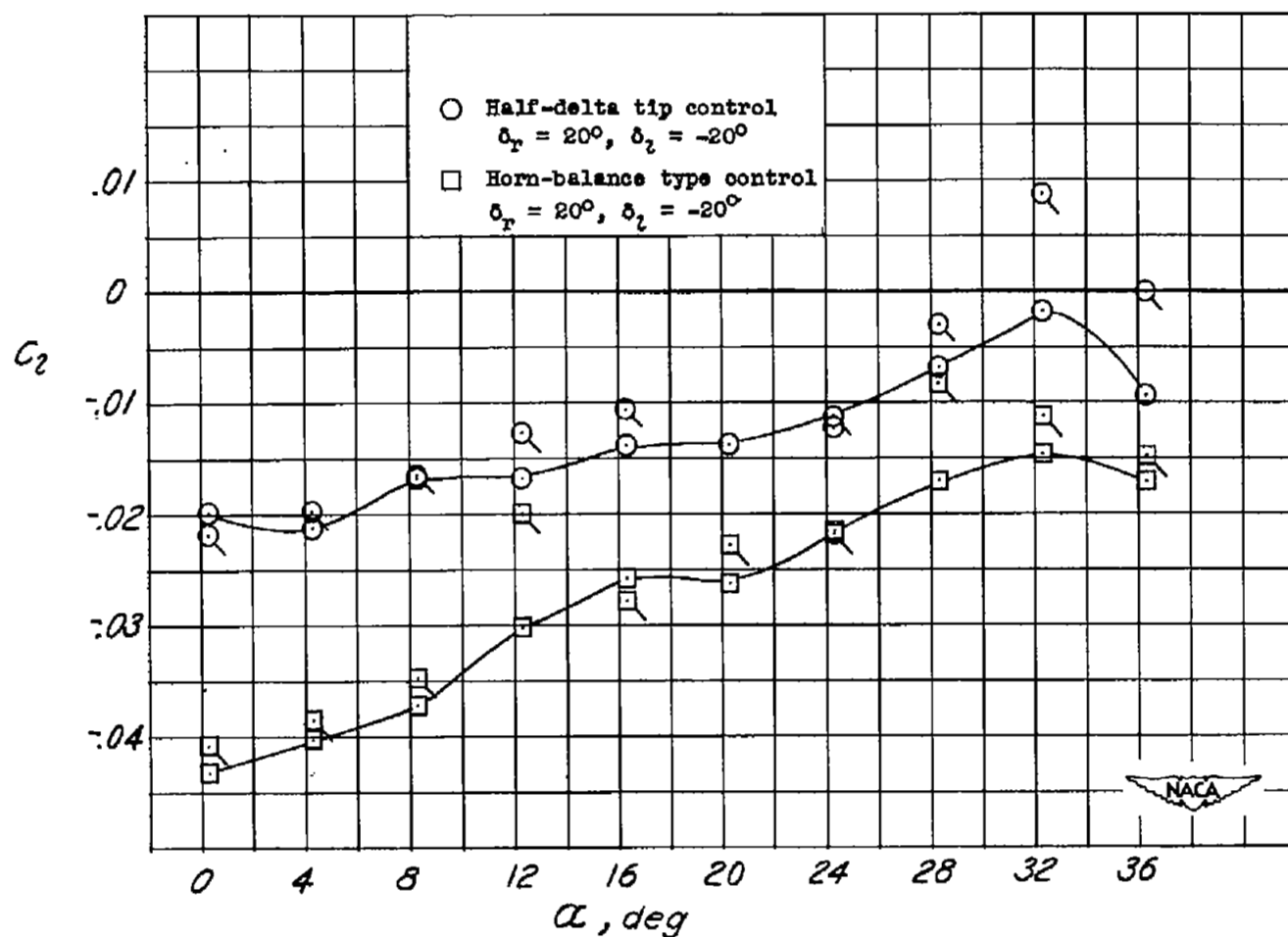
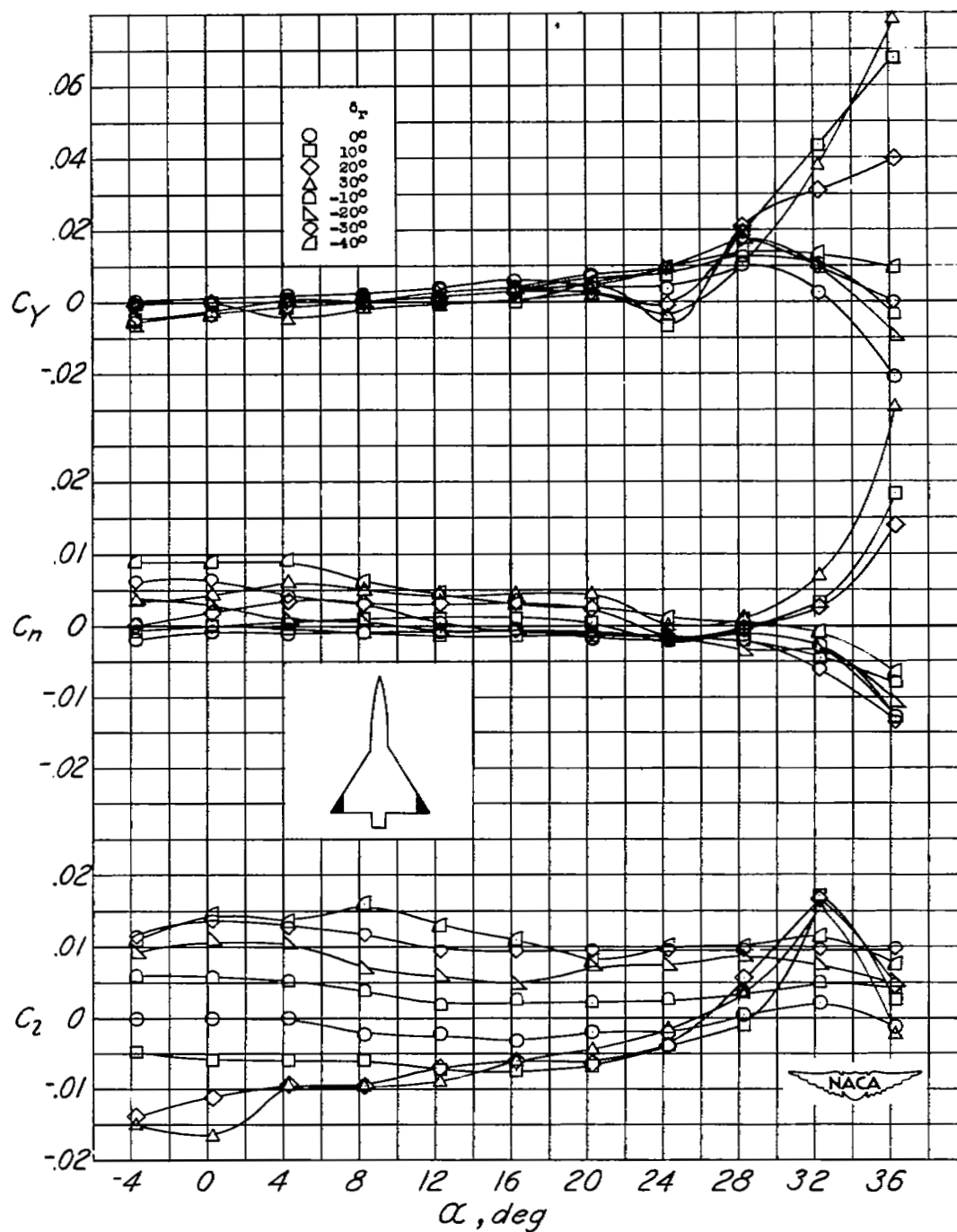


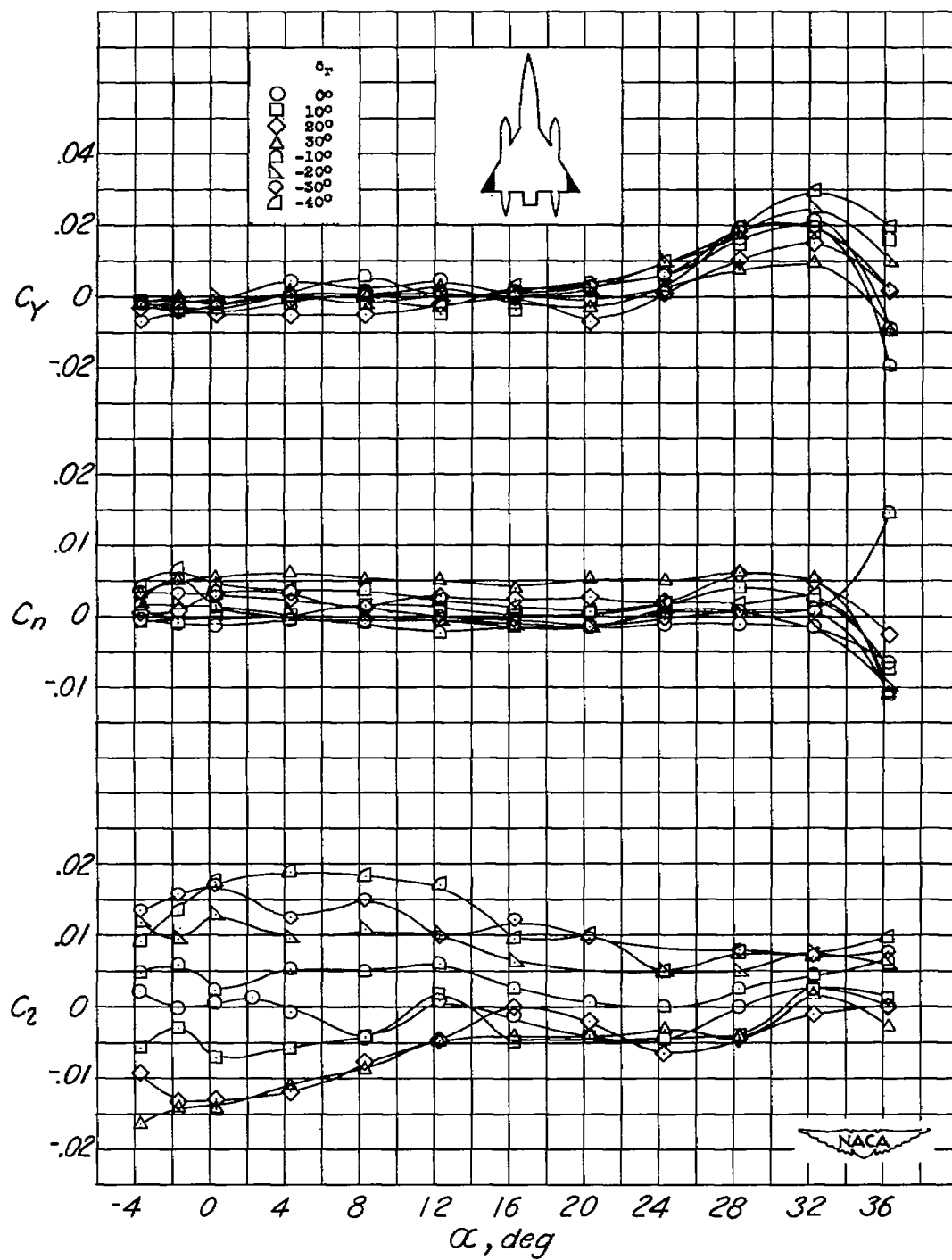
Figure 11.- Comparison of total rolling-moment coefficients for differentially deflected controls with those computed from the right semispan control deflections. Flagged symbols indicate the sum of the rolling moments when the controls are singly deflected.



(a) Configuration A.

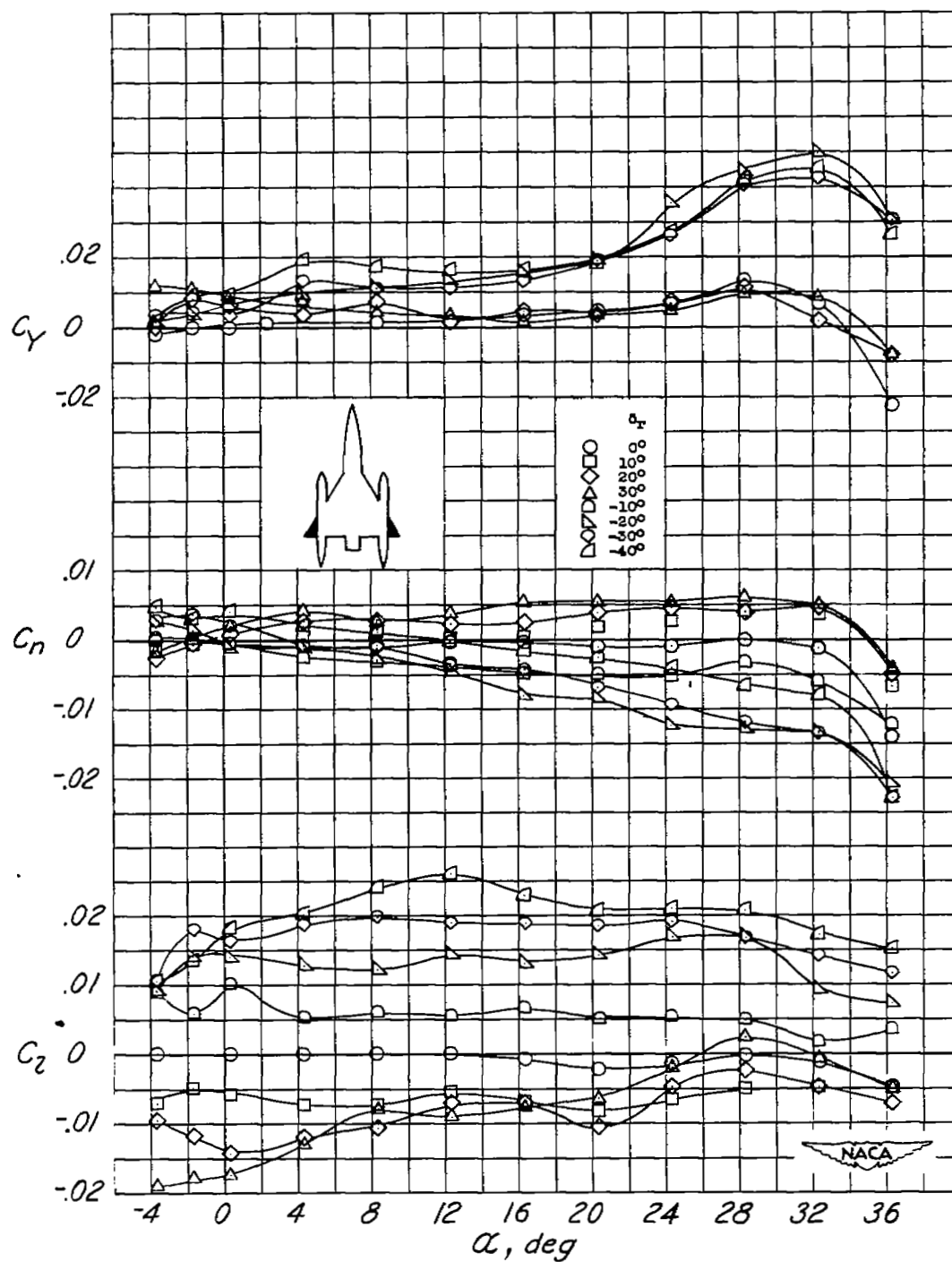
Figure 12.- Variation of  $C_L$ ,  $C_n$ , and  $C_m$  with angle of attack for the delta-wing model with half-delta and horn-balance-type controls.





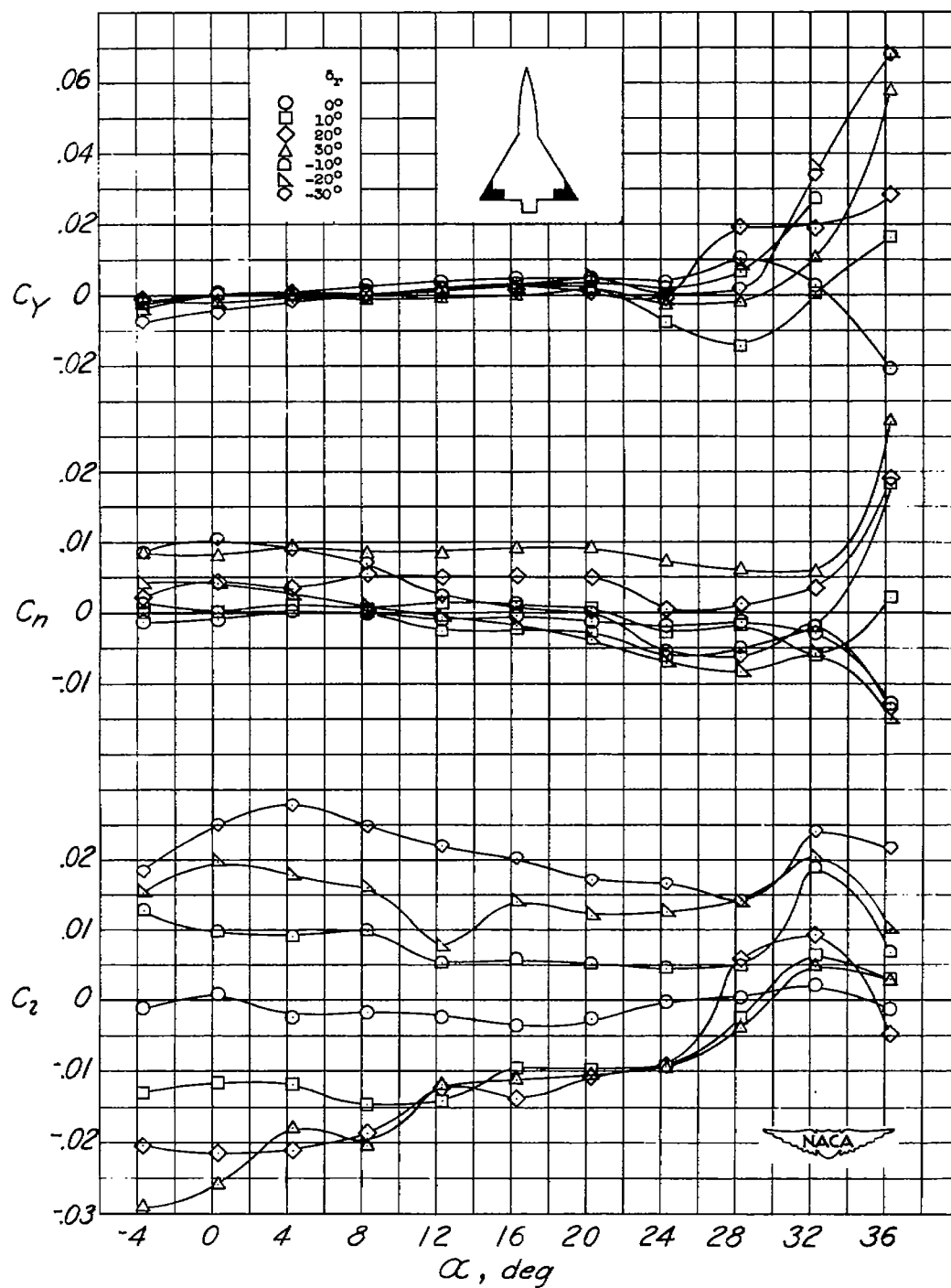
(b) Configuration A-48.

Figure 12.- Continued.



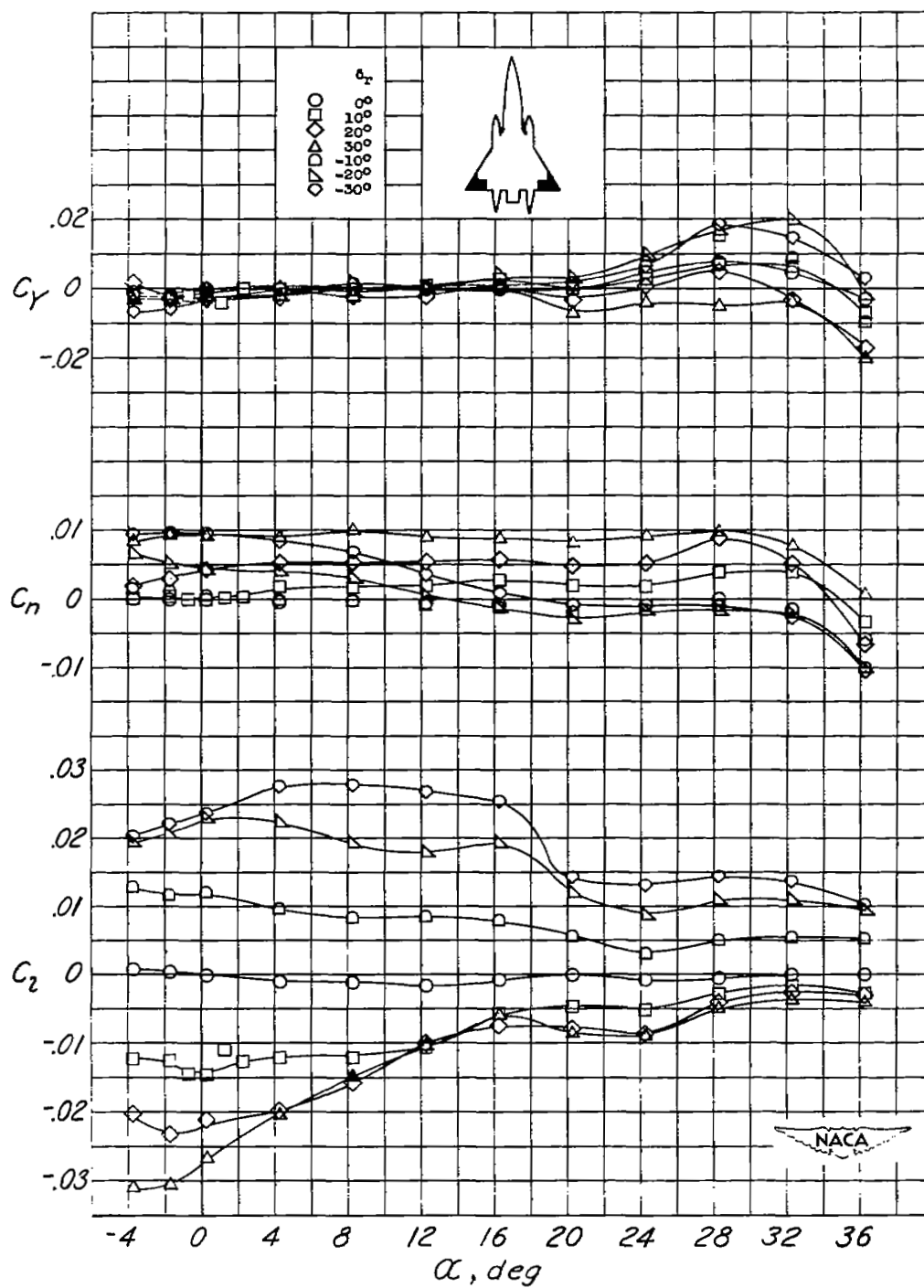
(c) Configuration A-67.

Figure 12.- Continued.



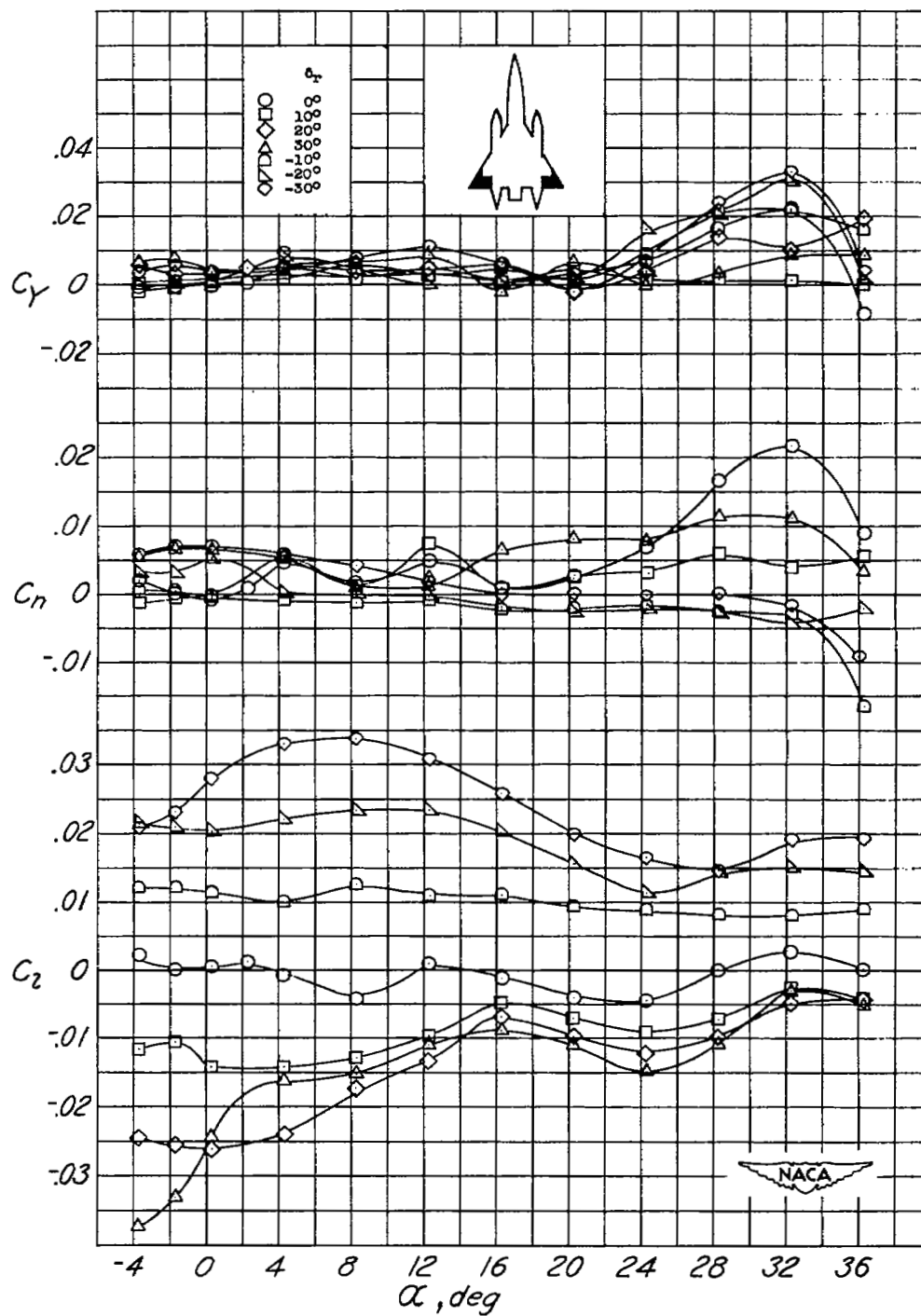
(d) Configuration B.

Figure 12.- Continued.



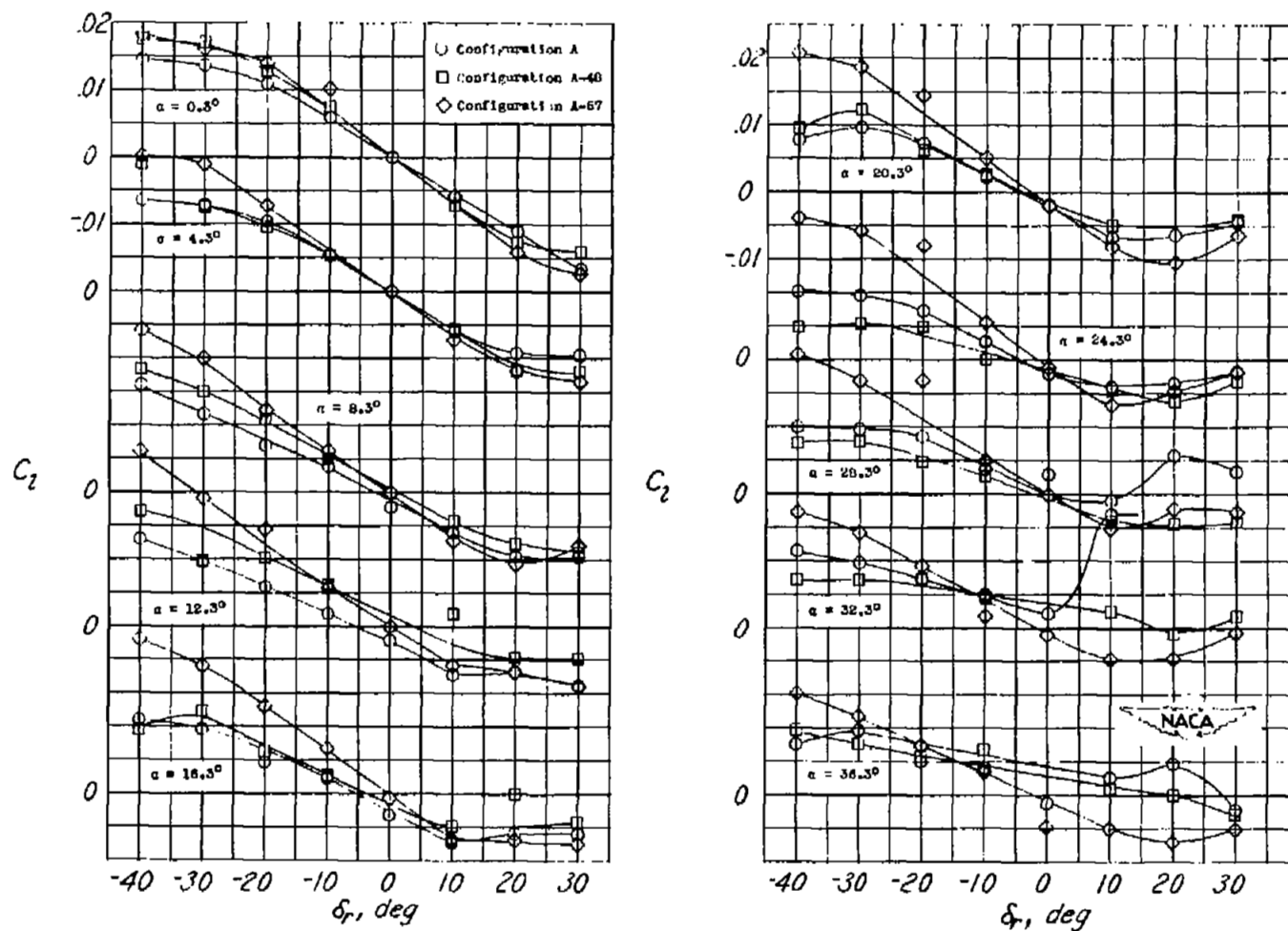
(e) Configuration B-33.

Figure 12.- Continued.



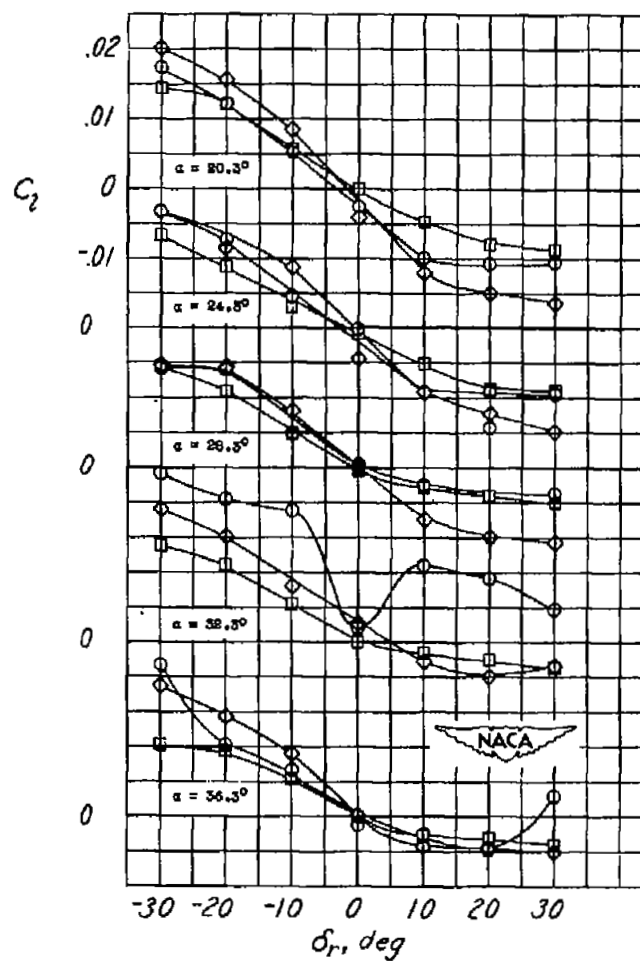
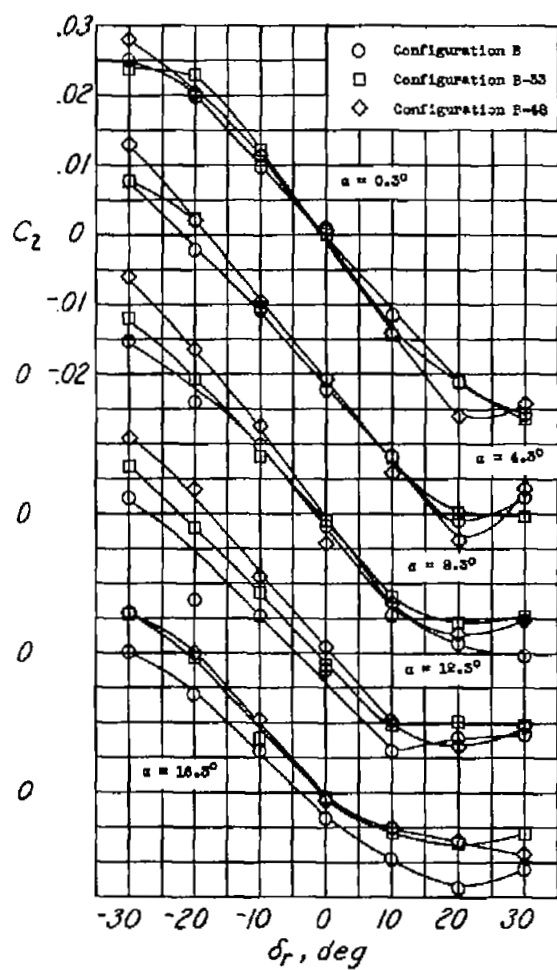
(f) Configuration B-48.

Figure 12.- Concluded.



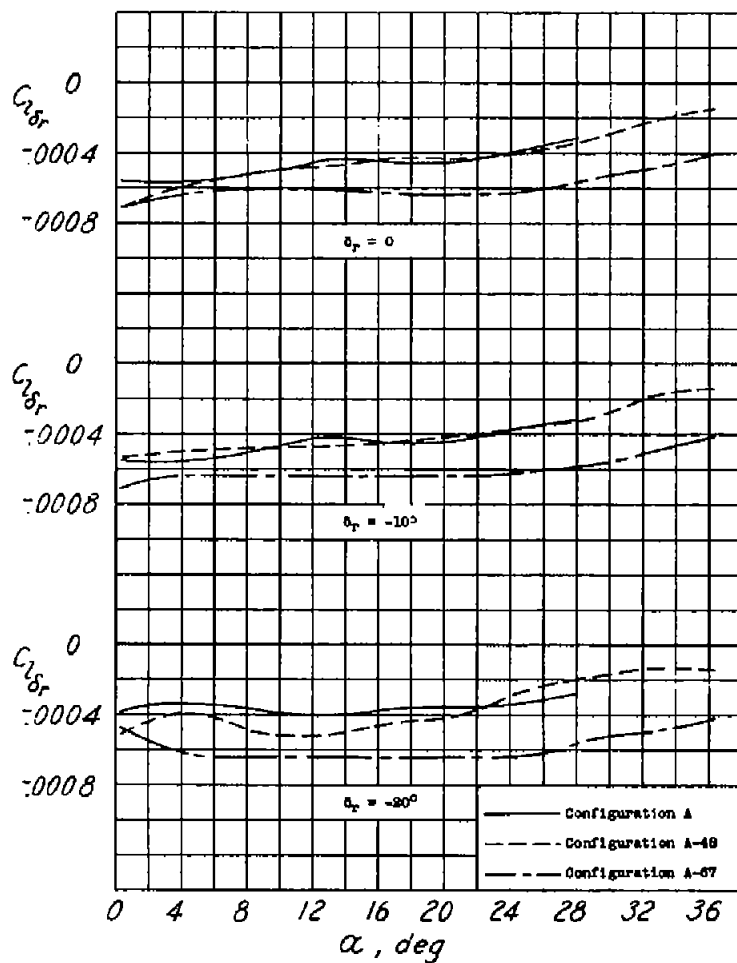
(a) Half-delta tip control.

Figure 13.- Variation of rolling-moment coefficient  $C_l$  with control deflection at several angles of attack.

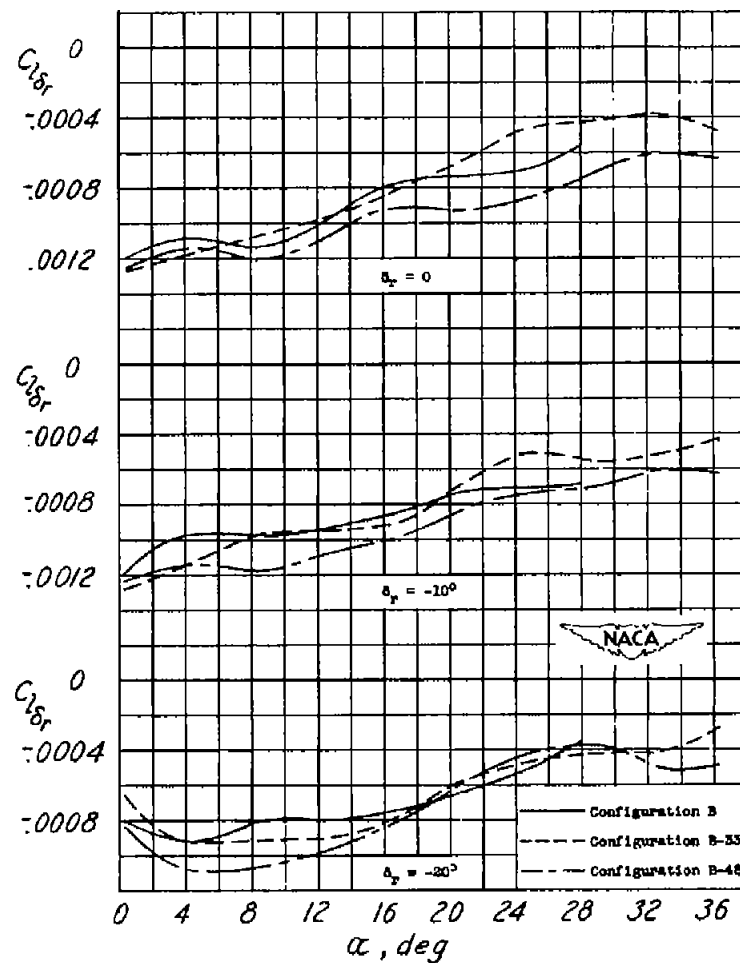


(b) Horn-balance-type control.

Figure 13.- Concluded.



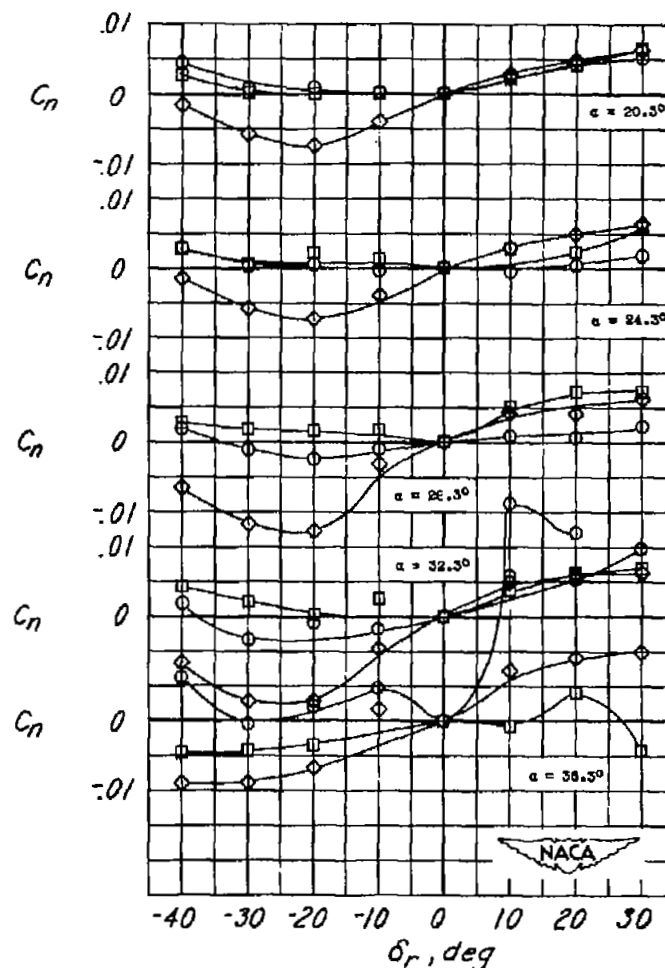
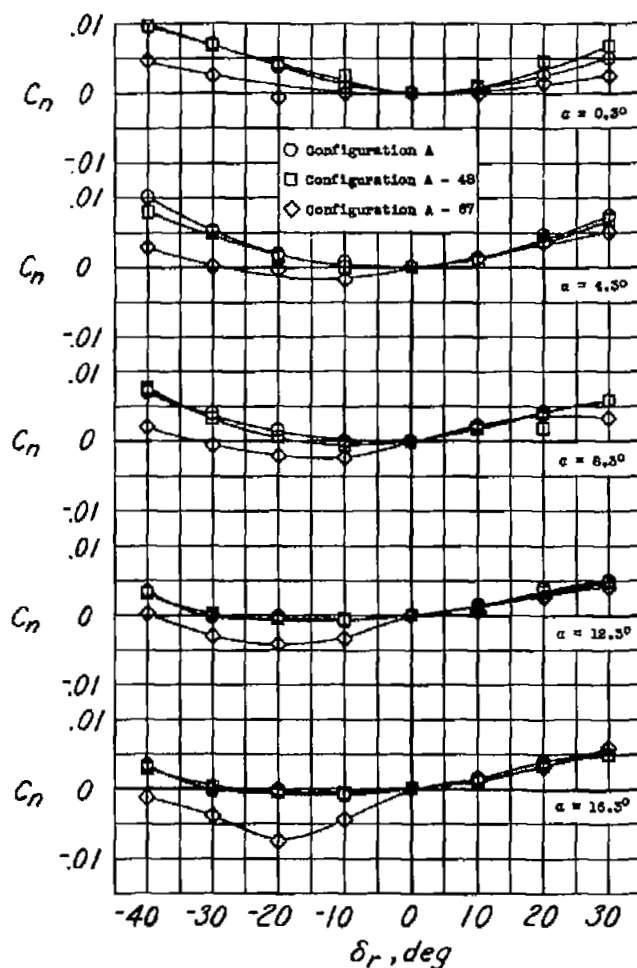
(a) Half-delta tip control.



(b) Horn-balance-type control.

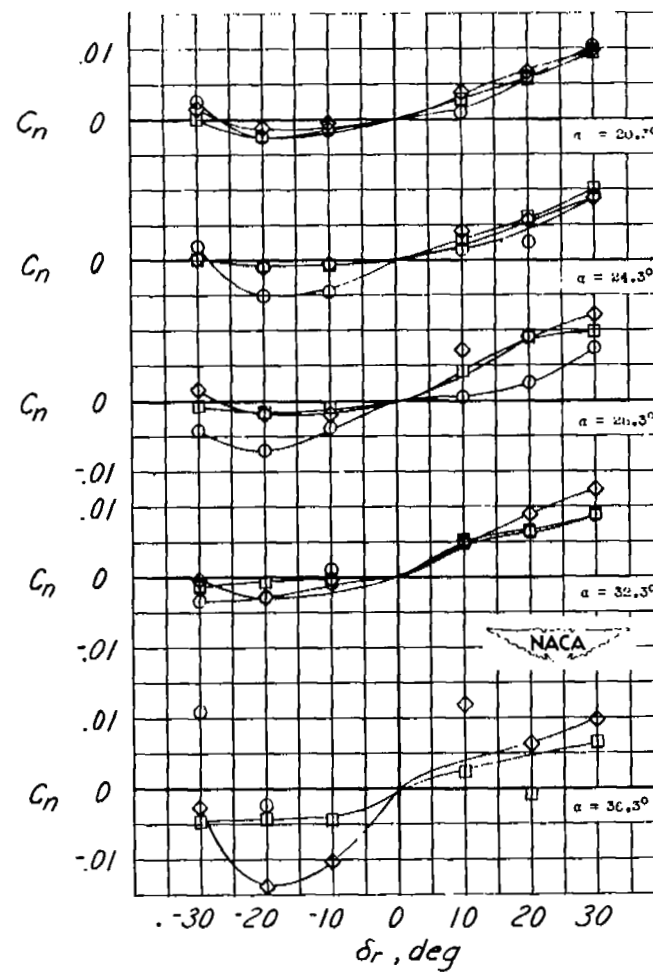
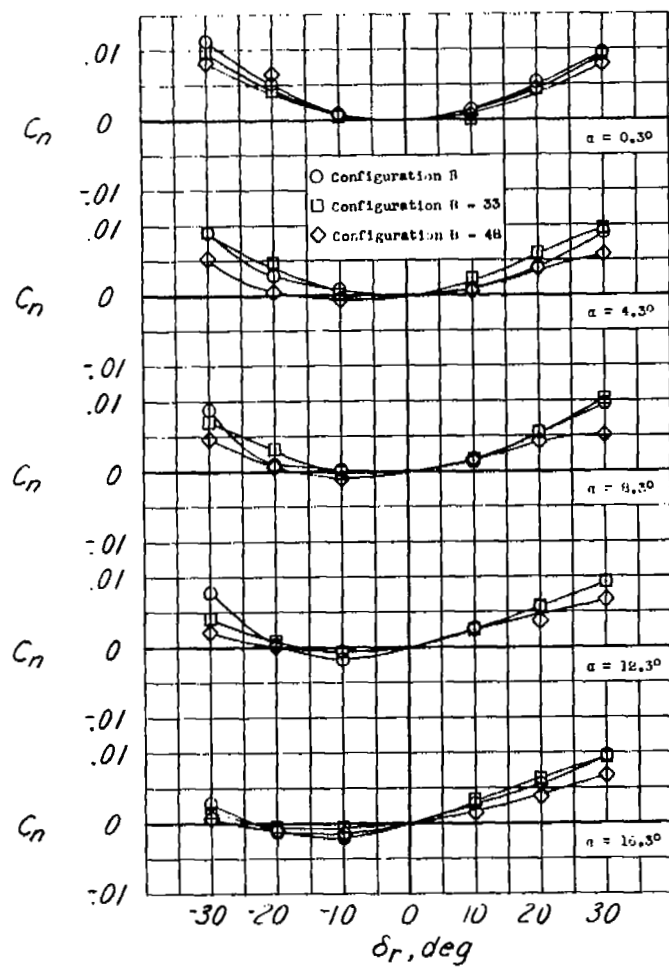
Figure 14.- Variation of the control parameter  $C_{l\delta_r}$  with angle of attack for the  $60^\circ$  delta wing with and without nacelles.





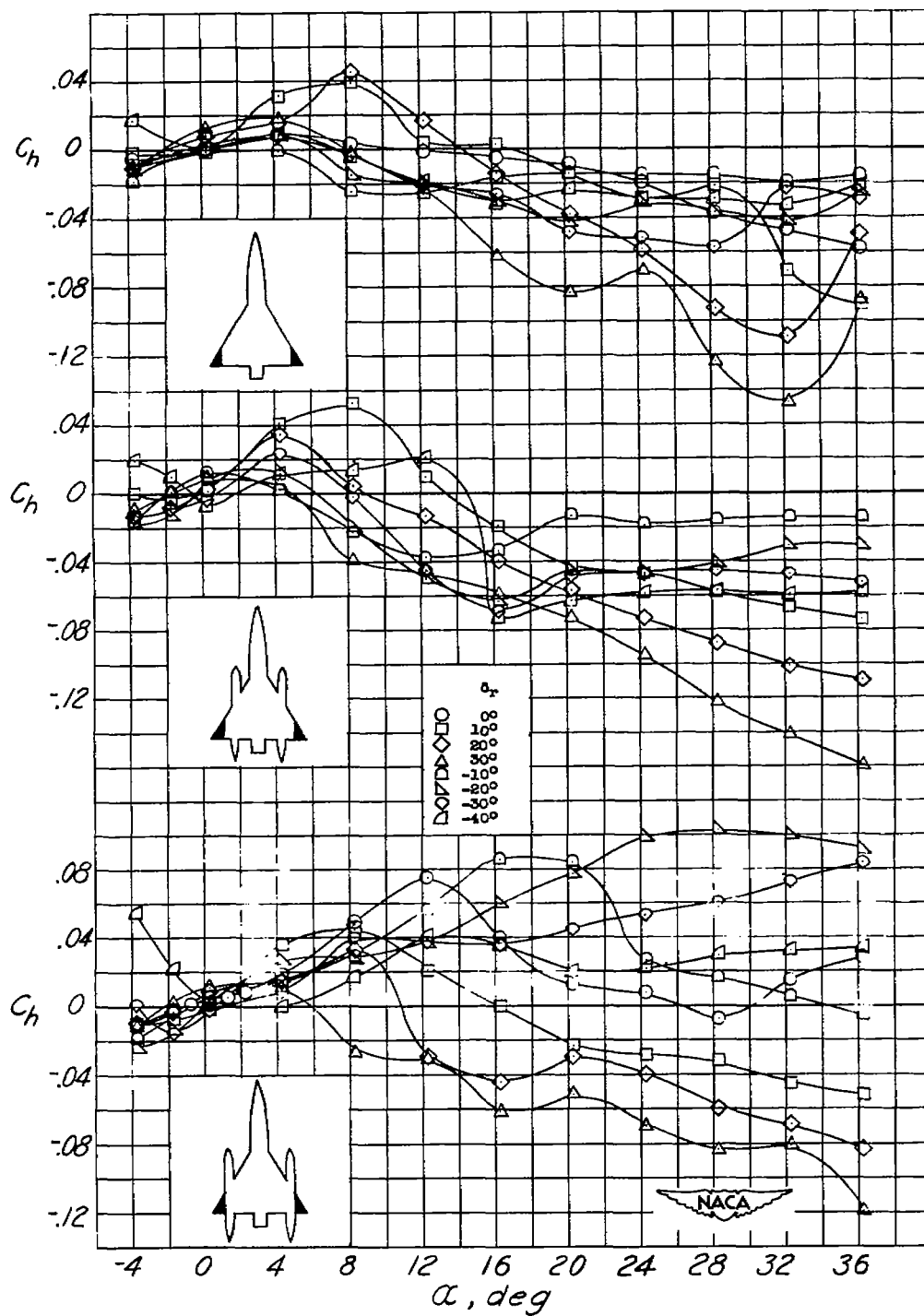
(a) Half-delta tip control.

Figure 15.- Variation of yawing-moment coefficient  $C_n$  with control deflection at several angles of attack.



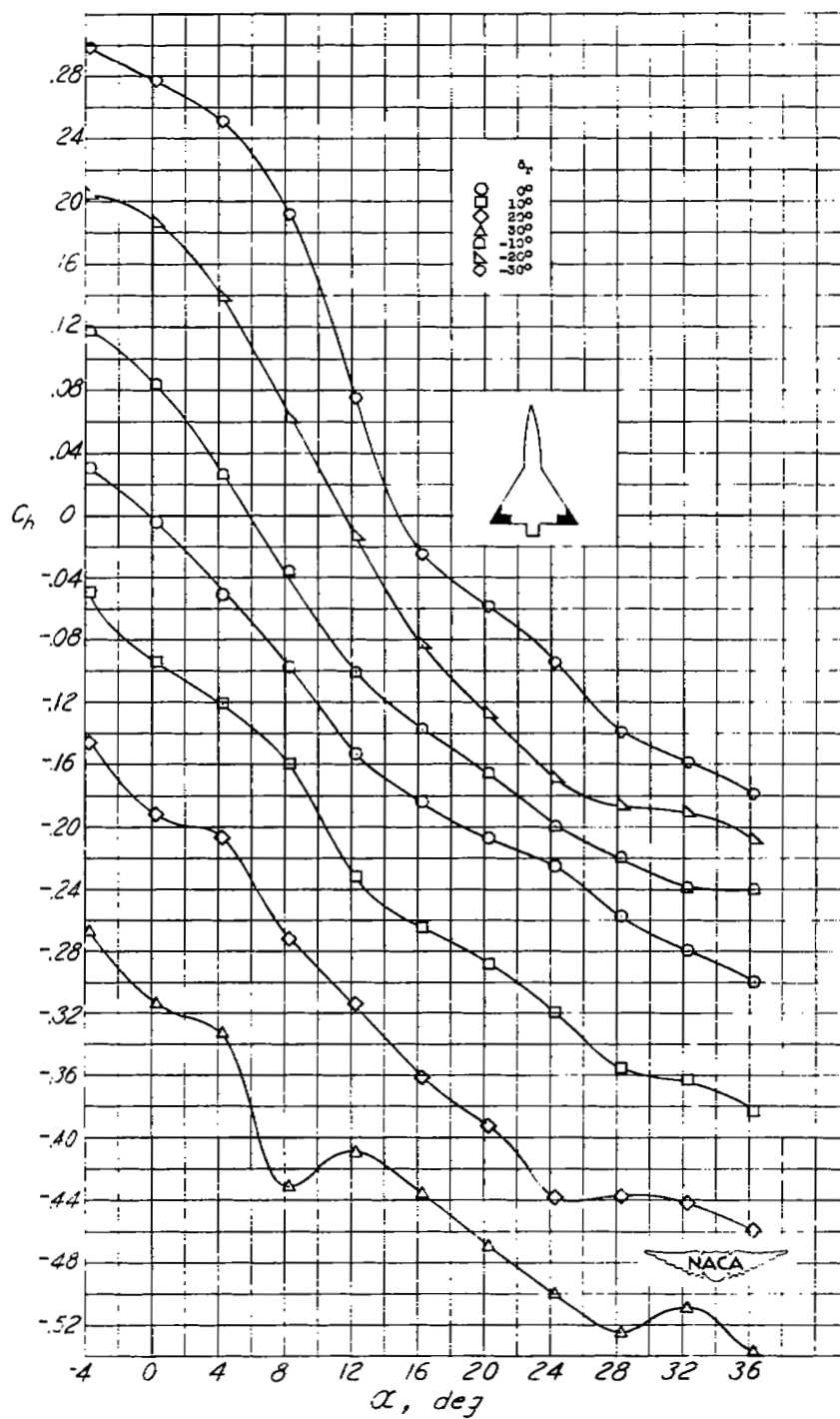
(b) Horn-balance-type control.

Figure 15.- Concluded.



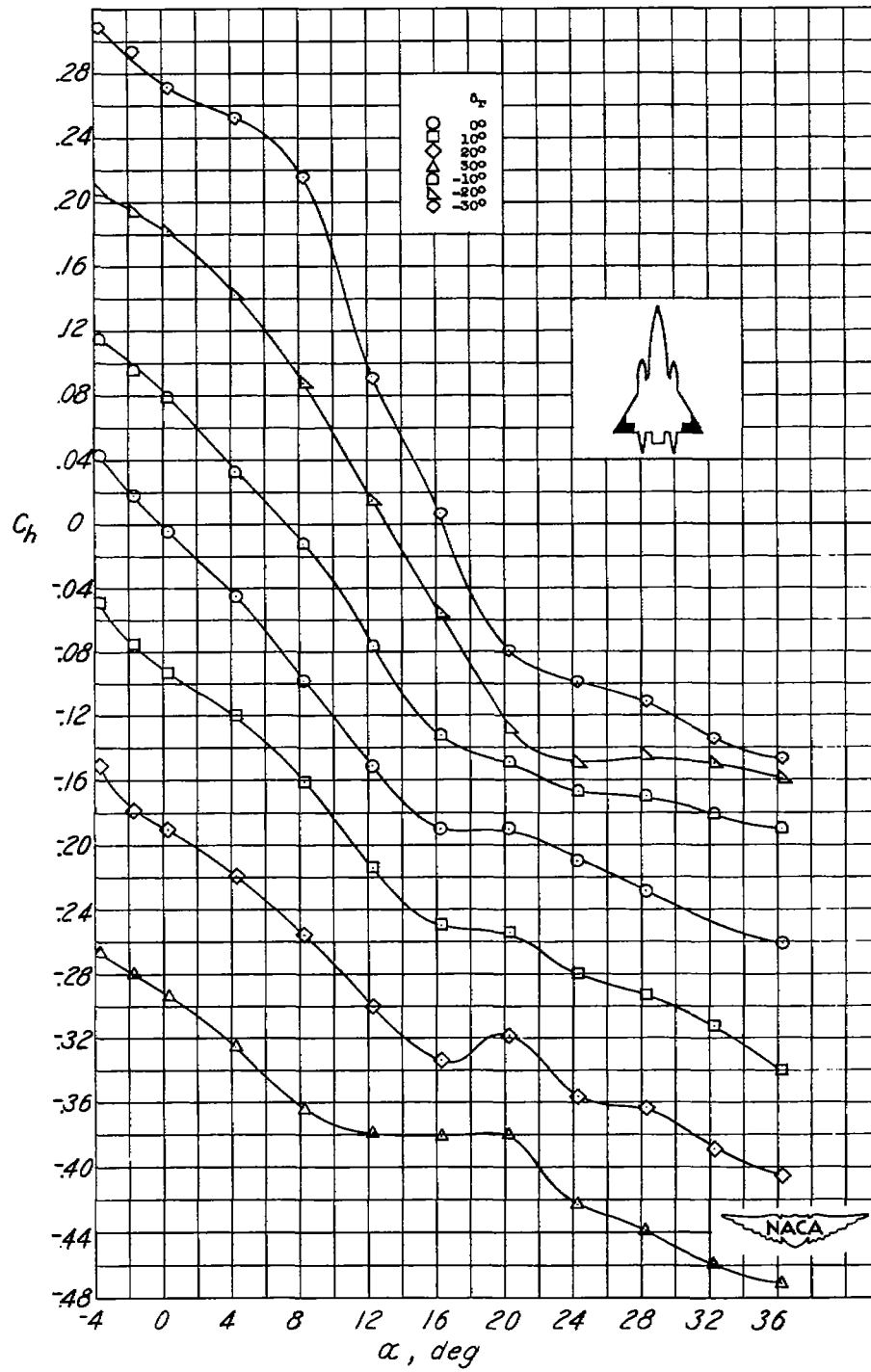
(a) Half-delta tip controls.

Figure 16.- Variation of hinge-moment coefficient  $C_h$  with angle of attack.



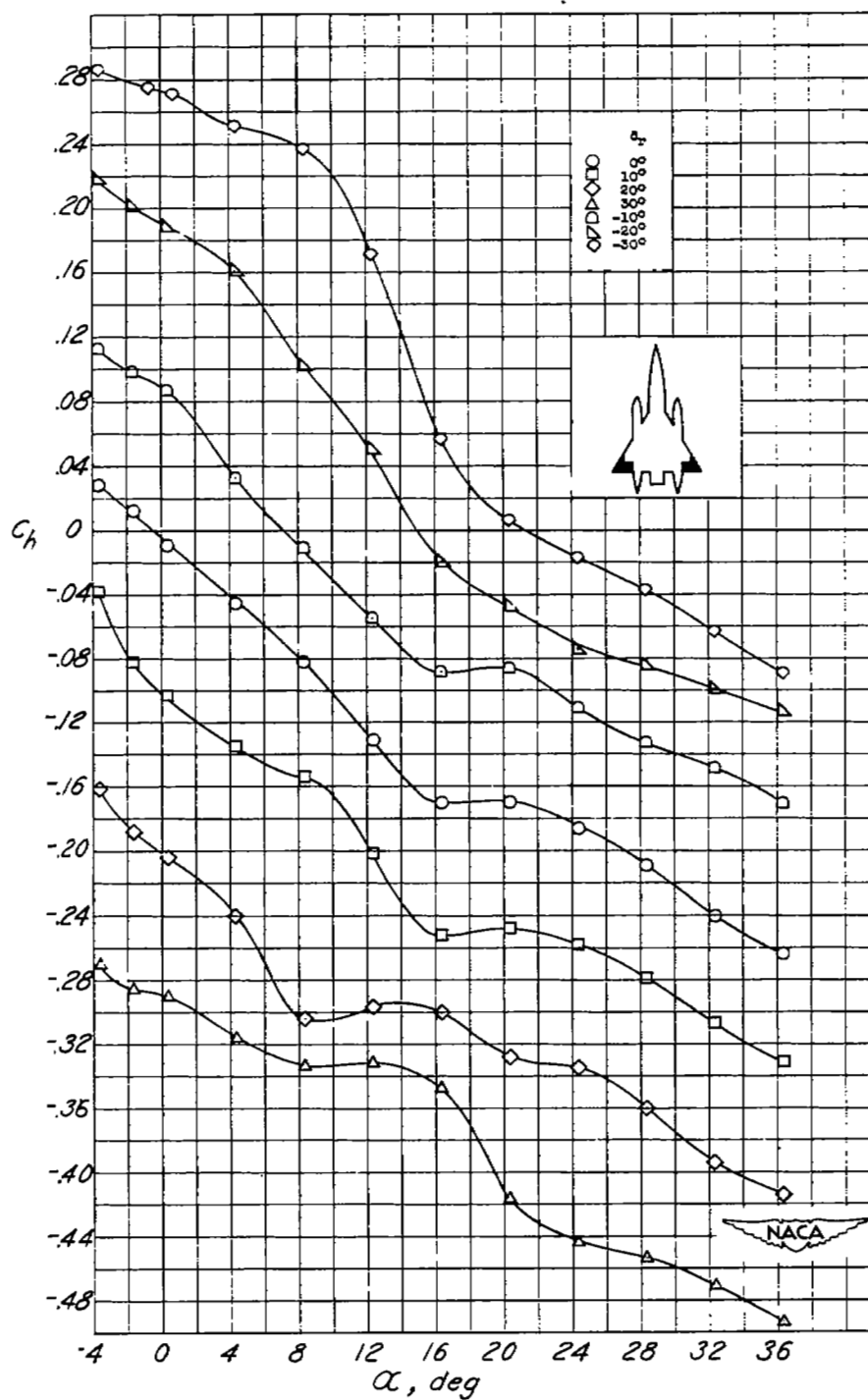
(b) Configuration B.

Figure 16.- Continued.



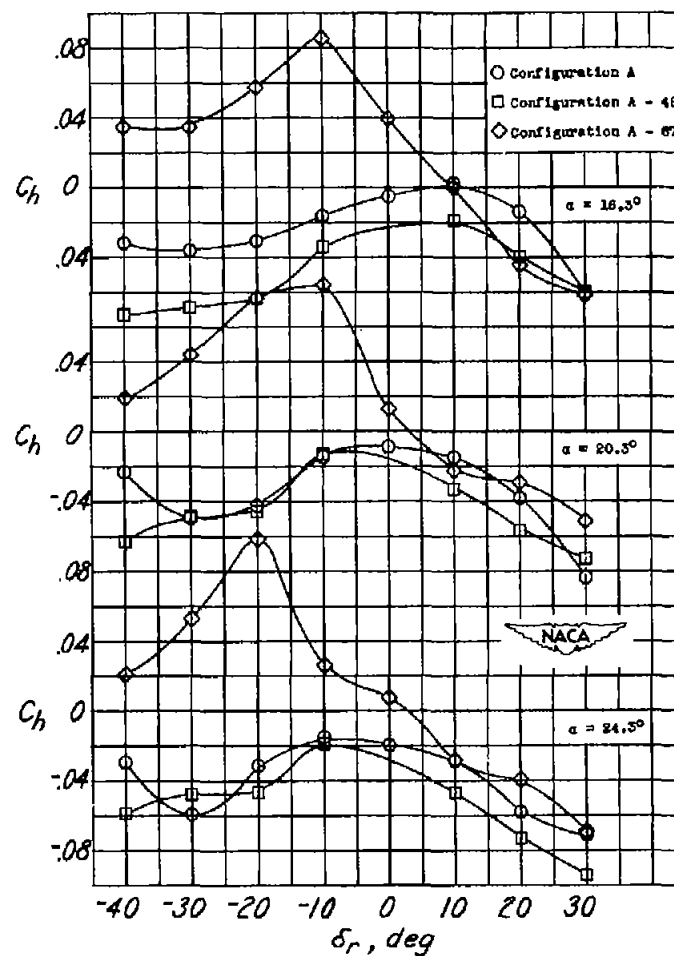
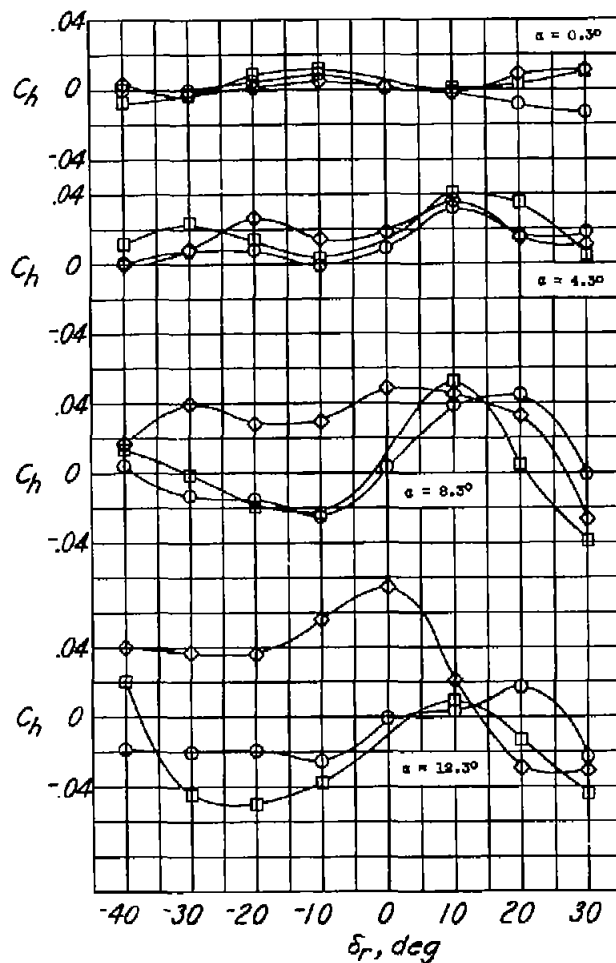
(c) Configuration B-33.

Figure 16.- Continued.



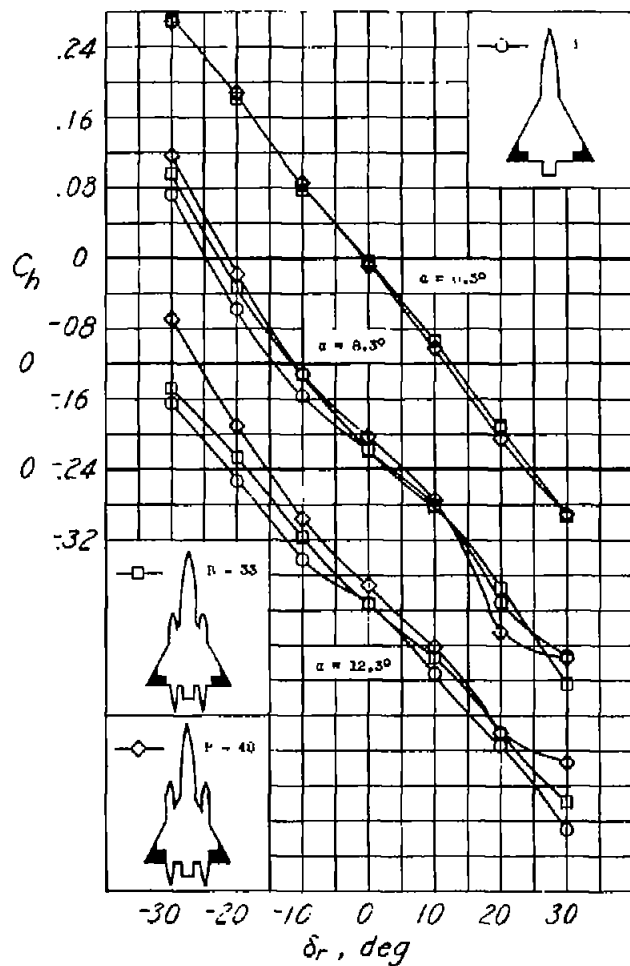
(d) Configuration B-48.

Figure 16.- Concluded.



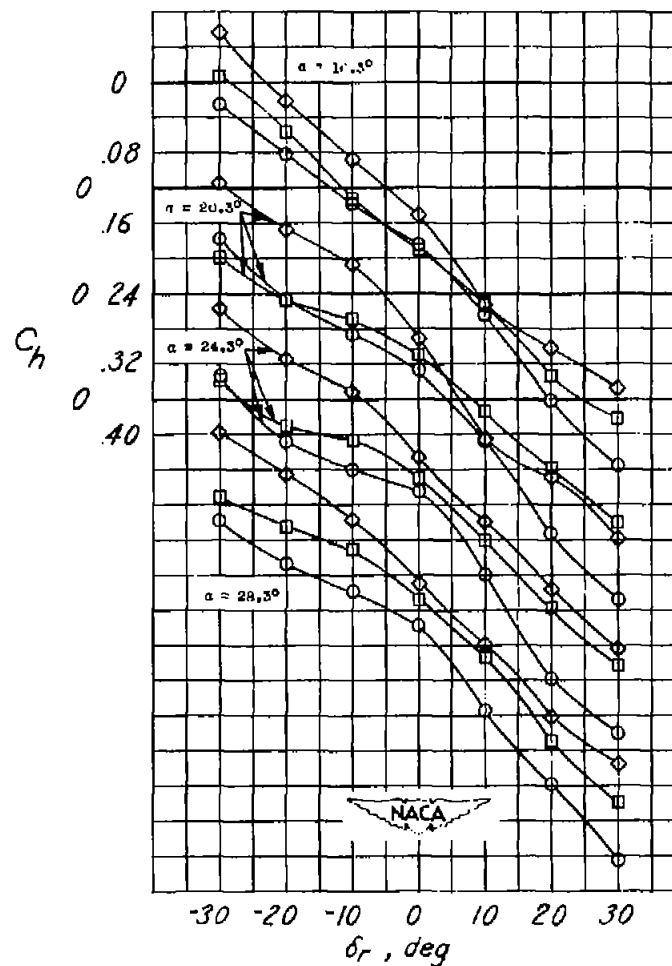
(a) Half-delta tip control.

Figure 17.- Variation of hinge-moment coefficient  $C_h$  with control deflection.



(b) Horn-balance-type control.

Figure 17.- Concluded.





SEC

NASA Technical Library



3 1176 01436 9814

INFORMATION  
AL

~~CONFIDENTIAL~~